行政院國家科學委員會專題研究計畫 期中進度報告

民生網路之前瞻研究--總計畫(1/2)
期中進度報告(完整版)

計 畫 類 別 ： 整合型
計 畫 編 號 ： NSC 95-2219-E-002-022-
執 行 期 間 ： 95 年 08 月 01 日至 96 年 07 月 31 日
執 行 單 位 ： 國立臺灣大學電信工程學研究所

計 畫 主 持 人 ： 陳光禎
共 同 主 持 人 ： 許大山

處 理 方 式 ： 期中報告不提供公開查詢

中 華 民 國 96 年 05 月 31 日

行政院國家科學委員會補助專題研究計畫 ■ 成 果 報 告
□期中進度報告

民生網路之前瞻研究-總計畫

計畫類別：□ 個別型計畫　　■ 整合型計畫
計畫編號：NSC　95－ 2219 － E － 002 － 022　－
執行期間：　95　年　8　月　1　日至　96　年　7　月　31　日

計畫主持人：陳光禎 教授
共同主持人：許大山 教授
計畫參與人員：　朱峰森 孔令宏 連紹宇 余仲鎧 梁育嘉 彭宇正
沈瑞欽

成果報告類型(依經費核定清單規定繳交)：□精簡報告　■完整報告

本成果報告包括以下應繳交之附件：
□赴國外出差或研習心得報告一份
□赴大陸地區出差或研習心得報告一份
□出席國際學術會議心得報告及發表之論文各一份
□國際合作研究計畫國外研究報告書一份

處理方式：除產學合作研究計畫、提升產業技術及人才培育研究計畫、列管計畫及下列情形者外，得立即公開查詢
□涉及專利或其他智慧財產權，□一年□二年後可公開查詢

執行單位：

中　華　民　國　95　年　5　月　30　日

中英文摘要、關鍵字與目錄

摘要：

民生網路已被視為未來無線通訊主要發展方向之一，許多先進的無線通訊科技皆逐漸的被應用在民生網路上。因此，民生網路將成為無線通訊科技最主要的應用領域之一。在本整合型計畫中，我們主要針對三項民生網路中重要的議題進行研究與討論。分別為三個子計畫：

1. 民生網路的服務品質控制機制（子計畫一）
2. 可重組式整合多模數位傳輸發展平台（子計畫三）
3. 多標準共存之可調無線介接與正交分頻（子計畫五）

同時，我們也提出基於 802.16e 正交分頻多重存取上之多媒體傳輸系統實作原型，可作為未來實現驗證理論之平台。三個子計畫之研究摘要如下所示。

子計畫一：

網路型民生系統與裝置的需求正快速的成長。無論是在家庭中、在車上、還是玩樂或工作中，常使用網路的人皆想要系統與裝置間良好的合作以提供娛樂、資訊與通訊。為了符合各式多媒體服務的要求，適當的服務品質保證機制是急切需要的。

在這兩年的計畫中，我們致力於提出能夠提供採用不同無線技術(包括 WiMAX, UWB 和 multihop WLAN)的民生網路服務品質保證的機制。我們採用跨階層的方法且排程、無線電資源管理與媒體存取控制的問題皆以我們之前的結果加以解決。

子計畫三：

現代化的消費性電子產品已廣泛地為大眾所使用。我們可以預期在未來使用者會有各式各樣的數位設備，而這些設備需靠好的通訊鏈結來達成其功能或資料傳遞；而能夠提供高傳輸量與高可靠度的無線通訊技術正可以滿足這些需求。在前一年的計畫當中，我們已經對WiMAX與IrDA通訊標準作一些深入的探討。在今年的計畫當中，我們將專研於紅外線無線通訊的效能提昇上。

無線紅外線傳輸為適用於未來民生網路的傳輸技術介面之一。在前一年的計畫當中，我們研究了紅外線無線通訊系統的系統效能表現。我們分析了在無線光通訊系統上有符號間干擾（ISI）與高斯白雜訊（AWGN）的情形下，使用單載波頻域等化技術（SC-FDE）在訊號強度調變/直接偵測(IM/DD)之通道上的效能表現。這樣的系統可以有良好的功率效益，且在等化器的實現上複雜度很低。在今年度的計畫之中，我們進一步研究紅外線無線通訊系統，在以提供更高的資料傳輸率的目標下所會遇到的課題。

VFIr標準為IrDA過去所制定之標準，可以提供到每秒16MB的資料傳輸率。VFIr標準採用了HHH(1,13)碼來避免掉符元間干擾的問題。然而這樣的設計不能滿足很多應用上更高資料傳輸率的需求。另一個制定中的標準UFIr，目標為要達到每秒100MB的傳輸速率。為了要

達到如此高的傳輸率，勢必要採用更寬頻的信號來傳輸，此時符元間干擾的問題會變的更加明顯且不能單單利用 HHH 碼的特性來避免掉此符元間干擾的效應。而今年的計畫目標即為提供一些解決此問題的接收端設計方案。

在今年度的計畫當中，我們研究了許多可能的方案來對付在IrDA HHH(1,13)編碼系統下遇到的符元干擾問題。在此報告中我們也會討論可應用在此系統的同步等化解碼演算法。但通常最佳同步等化解碼演算法的複雜度相當高，故我們也提出一些接近最佳效能表現但低複雜度的演算法。此低複雜度的演算法可以直接從 HHH(1,13)碼的軟性解碼器直接修改，而不需要增加其對應籬笆編碼圖上的狀態數。模擬的結果告訴我們此方法的確可以達到相當良好的性能表現。此外，基於我們提出的低複雜度演算法，我們也提出對應的碼設計條件，以期讓效能表現的損失降到最低。

子計畫五：

在這民生網路子計畫中，我們對民生網路（Consumer networks）的定義為，它必需能夠處理操作在同一個頻帶的多種不同通訊標準，包括在同一個裝置或在電波接受範圍之內的通訊環境。而在多種具有潛力的無線網路標準中，正交分頻多工無線區域網路系統(OFDM WLAN）、WiMAX 無線技術、以及使用多頻帶正交多頻分工（Multi-band OFDM）之超寬頻系統（UWB）被選為討論的對象。

因為這些系統都架構在正交分頻多工技術上，所以有必要針對影響系統效能的不理想特性作分析。相位雜訊在正交分頻多工技術中是一個主要的議題。本期計畫中，我們建立了相位雜訊的模型，並在正交分頻多工或是正交分頻多工多重存取的上行鏈路環境中估測相位雜訊。

此外，對於我們所提出之民生網路系統架構中之連結層作了探討。多個具有無線網路聯結功能的終端設備，在沒有基礎建設的情況下，其間可能建立無線隨意網路。而在無線隨意網路裡的節點通常會被要求以最小的功率來傳送資料，同時又要顧到傳送距離來達到網路之連通性。為了以更具功率效率的方法來控制網路拓撲架構，我們探討在無線隨意網路中之最佳傳送距離(或發射功率)、服務範圍的大小以及網路連通性三者彼此之間的關係。

本總計畫報告為整合三個子計畫之研究內容而呈現之。

Abstract

Consumer networks have been considered as a major development direction of future wireless communications. Many advanced wireless communication technologies are gradually be applied on consumer networks. Therefore, consumer networks will become one of the most important application areas of wireless communication technologies. In this integrated project, we focus the research and discussions on three important topics in consumer networks, and three subprojects are included.

1. The mechanism of quality of service (QoS) control in consumer networks. (subproject 1)
2. Software defined reconfigurable platform for integrated multimode modem. (subproject 3)
3. Adaptability and re-configurability of radio design to operate in co-existence multi-standard environments. (subproject 5)

We also propose an implementation prototype of wireless multimedia transmission over OFDMA system based on 802.16e, and which can be used as a platform for the realization of developed theories. Abstracts of three subprojects are following.

Subproject 1:

The demand for networked consumer systems and devices is large and growing rapidly. At home, in a car or truck, at work or at play, Internet citizens want transparent internetworking for the systems and devices that provide entertainment, information, and communications. In order to meet the quality of service (QoS) requirement for a variety of multimedia services, proper QoS mechanisms are urgently required.

In this two-year project, we aim to propose mechanisms that enable QoS for consumer networks adopting a variety of wireless technologies, including WiMAX, UWB, and multihop WLAN. A cross-layer approach is adopted and the issues of scheduling, radio resource management, and medium access control are addressed based on our previous results.

Subproject 3:

Modern electronic consumer devices are widespread use today. We can expect that consumers will own more and more devices and appliances that depend on an effective connection with the outside world for its proper function. Wireless communication technologies that can provide high data-rate and high reliability are very suitable for such demands. In the last year, we had investigated both WiMAX and IrDA systems. In the project this year, we focus on the performance enhancement of wireless infrared technology.

IrDA (Infrared Data Association) connection technology is a good candidate for future consumer network. In the project last year, we had examined IrDA-based systems and their system performance. We had shown that SC-FDE (Single carrier modulation with frequency

domain equalization) is a technique suitable for optical communication systems using intensity modulation with direct detection (IM/DD) in the presence of additive white Gaussian noise. We derived the performance when SC-FDE and pulse position modulation (PPM) are adopted to combat ISI for IM/DD channels. Such a system enjoys the average power efficiency of PPM and the low complexity equalization of SC-FDE. Following the result of the first year project, we keep studying on the IrDA systems that can provide higher data-rate support.

Very Fast Infrared (VFIr) was promoted by the IrDA for data rate of 16Mb/s. VFIr adopts HHH (1,13) code (a kind of run length limited/RLL code) to avoid ISI problems. However, such transmission rate cannot satisfy the demand of numerous modern applications. Another protocol UFIr (Ultra Fast Infrared), which is in development, will provide data rate up to 100Mb/s. To achieve such high data-rate transmissions, wide-band signals will be used. Then the effect of component and channel induced inter-symbol interference (ISI) will become more and more crucial and cannot be compensated easily only by HHH-code's property. Therefore, one may introduce an equalizer to deal with ISI problem, since the ISI-avoided property of HHH code does not work anymore. The goal of this year is to provide solutions to deal with ISI problems.

In this project, we examine several possible approaches to deal with ISI problems in IrDA RLL-coded systems; joint equalizing and decoding methods for such systems are also discussed. Since the computational complexity of optimal joint receiver is quite high, we also provide sub-optimal algorithms, which are directly modified from the soft-decoder for HHH code without increasing the number of states of the encoding trellis. The simulation results show that our algorithm does yield good performance. Based on our sub-optimal algorithm, we provide the corresponding code design criterion so that the performance penalty can be further reduced.

Subproject 5:

In the project of Consumer networks, the term “”consumer networks” is promised to deal with multiple standards operating in the same frequency band, either within the same device or with a radio range. Among many potential wireless networks standards, OFDM WLAN, WiMAX, and UWB using multi-band OFDM are selected to be discussed.

Because that these three systems are based on OFDM technique, there is a need to analyze the non-ideal characteristics of such technique. Phase noise is the main issue in OFDM technique. In this subproject we build up the model of phase noise and estimate the phase noise in uplink OFDM/OFDMA.

Besides, we discuss the connectivity layer of system architecture for consumer networks. Plenty terminal equipments capable of wireless connectivity may construct wireless ad hoc networks under the situation of none infrastructure. Nodes in the wireless ad hoc networks are required to conserve the limited battery life with minimized transmission power. In addition, the wireless ad hoc networks are required to be connected. In order to control the topology structure in a power-efficient way, the discussion on relationships of the best transmission distance (or

transmission power), the coverage of the service and network connectivity is given.

This report is presented by integrating the research results of three subprojects.

目錄

子計畫一、民生網路的服務品質控制機制

I. 研究背景與目的

In this two-year project, we aim to propose mechanisms that enable QoS for consumer networks adopting a variety of wireless technologies, including WiMAX, UWB, and multihop WLAN. A cross-layer approach is adopted and the issues of scheduling, radio resource management, and medium access control are addressed based on our previous results.

In this year (i.e., the second year), we proposed a rate-adaptation mechanism for adjusting the modulation scheme of layer-encoded video stream to provide multicast video services over UWB systems. The purpose of the work is to provide a fast adaptation scheme while minimizing the computation complexity of the video server who offers the multicast video services. We further propose a location-independent scheduling mechanism (LISM) [1,2] that may work on top of *Ripple* [3] to resolve the location-dependent throughput problem for multihop WLAN systems. We further extend the concept of *Ripple* and proposed a new medium access control (MAC) protocol, named IWTRP [4], for a ring topology. Most of the results have been presented in IEEE conferences and some of the proposed mechanisms are being implemented in a micro-controller.

The work presented in this year is an extension of our previous work. In the last year, we have developed a dynamic rate selection (DRS) scheme for adjusting the modulation scheme of layer-encoded video stream for providing multicast video services over WiMAX systems. Different to the rate-adaptation mechanism proposed for UWB, the main purpose of the proposed rate-adaptation mechanism is to maximize the profit of the network operator while guaranteeing the QoS of video services for users located within the network.

In our previous work, we also proposed an enhanced MAC protocol [3], named *Ripple*, to enhance the attainable throughput for tree-based multihop WLAN networks. The multihop WLAN, also known as WiFi mesh network, has been standardized by IEEE 802.11s and aims to provide service for residential, office, campus/community/public access network, public safety, and military application environments. The following description identifies the main issues of wireless networking for residential application.

‘In the digital home usage model, the primary purposes for the mesh network are to create low-cost, easily deployable, high performance wireless coverage throughout the home. The mesh network should help to eliminate RF dead-spots and areas of low-quality wireless coverage throughout the home. High-bandwidth applications such as video distribution are likely to be used within a home network, thus high bandwidth performance will be very important for residential mesh networks. The most demanding usage of bandwidth in the mesh network is expected to come from device-to-device communication within the home, e.g. multi-media content distribution between different devices in the home. Mesh Points and Mesh APs may be implemented in dedicated AP devices, PCs, and high-bandwidth CE devices with line-power supply such as TVs, media center devices, and game consoles. STAs may be a combination of computing devices such as PCs, laptops, and PDAs, CE devices such as digital cameras, MP3

players, DVD players, and home automation devices such as control panels. In the short-term (3-5 years), the home network is expected to consist of a small number of Mesh APs/Mesh Points that are primarily dedicated devices or PCs. In the longer-term (5+ years), a larger number of CE devices are expected to become Mesh APs/Mesh Points, increasing the size of the mesh network over time. Some devices (e.g. battery powered CE devices) may be capable of operating as Mesh Points but require more conservative use of power than AC-powered Mesh Points. These low-power devices may optionally require Mesh Points to choose not to forward packets for other nodes in the network or to support a doze mode with lower duty cycle to conserve energy. A mesh network should be self-configuring to allow easy installation by non-technical consumers and ongoing operation without system administration. Mesh Points and Mesh APs may need to be configured as bridges to other LANs within the home, including, but not limited to, legacy Ethernet LANs, 802.15 WPANs, and legacy 802.11 WLANs. As mesh deployments become more popular in the future, the coexistence of multiple mesh networks deployed in neighboring homes of dense residential complexes (such as apartments and neighborhoods) will become an important factor for network performance. Residential home networks must be able to coexist with other mesh networks and BSS networks deployed in nearby houses. This may require dynamic, self-configuring adaptation of RF settings such as channel and TX power for effective radio resource sharing. This also means that residential network deployments will often have multiple overlapping security domains, requiring security protocols to protect communication from malicious users that may overhear data transmissions. [5]'

The description mentioned above was defined in the TGs usage model [5] for the residential environment. It can be found that the consumer network shares the same vision as that of mesh network in such an environment. Hence, we decide to extend the scope of the project and further develop QoS mechanisms based on this new technology.

II. 提出之方法

There are three methods proposed in this project. The first method is a dynamic rate selection (DRS) scheme proposed to support real-time video broadcasting services for consumer networks adopting ultra-wideband (UWB) technology. The DRS scheme aims to maximize the average quality of clients by adjusting the modulation scheme of UWB according to the location distribution of clients. The computation complexity of the DRS is then further reduced by utilizing the characteristic of DRS. Simulation results demonstrate the effective of the proposed scheme in various conditions. Details of the DRS will be elaborated in the remaining part of this section. The second method is a location-independent scheduling mechanism (LISM) [1,2] for resolving the location-dependent throughput problem for multihop WLAN systems adopting a tree topology. Details of the analysis and the application of the LISM can be referred to the Appendix A and B. We further proposed an improved wireless token ring protocol (IWTRP) [4] for multihop WLAN system adopting a ring topology.

In the following, we will briefly describe the basic concept of the dynamic rate selection (DRS) scheme. We consider MultiBand-Orthogonal Frequency Division Modulation (MB-OFDM) based USB system. The supported data rate and modulation scheme of MB-OFDM is listed in Table 1.

Data Rate (Mb/s)	Modulation	Coding Rate	Frequency-Domain Spreading (FDS)	Time-Domain Spreading (TDS)
53.3	QPSK	1/3	Yes	Yes
80	QPSK	1/2	Yes	Yes
106.7	QPSK	1/3	No	Yes
160	QPSK	1/2	No	Yes
200	QPSK	5/8	No	Yes
320	DCM	1/2	No	No
400	DCM	5/8	No	No
480	DCM	3/4	No	No

Table 1. The supported data rate and modulation scheme of MB-OFDM.

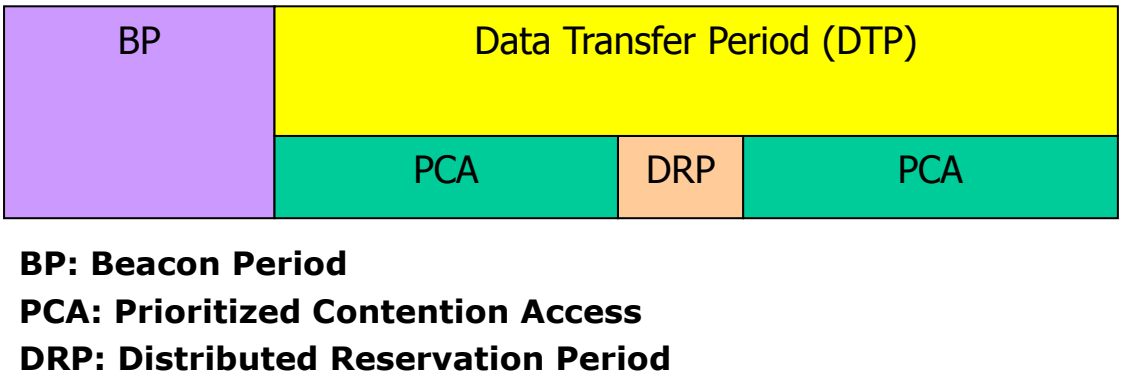

Fig. 1. The super-frame architecture of MB-OFDM MAC.

At the MAC layer, time is divided into super-frame with fix-duration. Each super-frame consists of a beacon period (BP) and a data transfer period (DTP), as shown in Fig. 1. The BP is used by the stations to announce its scheduling information. Each station may also estimate the signal quality of the other station and select a proper data rate based on the signal strength received in BP. DTP is used by stations to transmit their data packet. Both contention-based (i.e., PCA) and reservation-based (i.e., DRP) channel access mechanisms are supported by MB-OFDM MAC.

In this project, we focus on the multicast video services in residential environment adopting UWB transmission technology, as shown in Fig. 2. The video server is assumed to adopt scalable video coding that can encode the video streams into several layers, which includes one base layer (BL) and one or more enhancement layers (ELs). BL carries the fundamental information of the video stream and the remaining information is carried by the ELs. The receiver may have a better video quality if more enhancement layers are decoded. Note that, in scalable video coding, the information carried by higher layer cannot be retrieved if the lower layer information is corrupted. As illustrated in Fig. 2, in the residential environment, the signal quality of a receiving

consumer electronic device is highly dependent on its relative location to the video server. Hence, different devices may have different signal-to-noise-ratio (SNR) and packet error rate (PER) if a single modulation scheme is adopted. Hence, for each layer, the video server may choose a proper modulation scheme (or, equivalently, the transmission rate) to transmit its packets such that the average video quality experienced by all of the devices could be maximized. In the residential environment, each consumer electronic device may be portable and thus, the location of the device may be changed during the service period. Hence, the transmission rate of the server for each layer shall also be changed over time. As mentioned, in MB-OFDM, the video server can acquire the signal quality of each device and adjust its transmission rate in a frame-by-frame basis. In order to achieve the best performance, the video server may need to adjust the transmission rate frequently, which results in a high computation complexity. Therefore, a dynamic rate selection (DRS) scheme is proposed for the video server to adjust the modulation schemes for each layer but with reduced complexity.

DRS relies on the location distribution of the receiving devices, which can be estimated based on the signal qualities transmitted in BP. The most robust modulation scheme is used to transmit packets belonging to the BL in order to guarantee the minimum video quality for each device. For simplicity, a single EL is assumed herein and the result can be easily extended to accommodate several ELs.

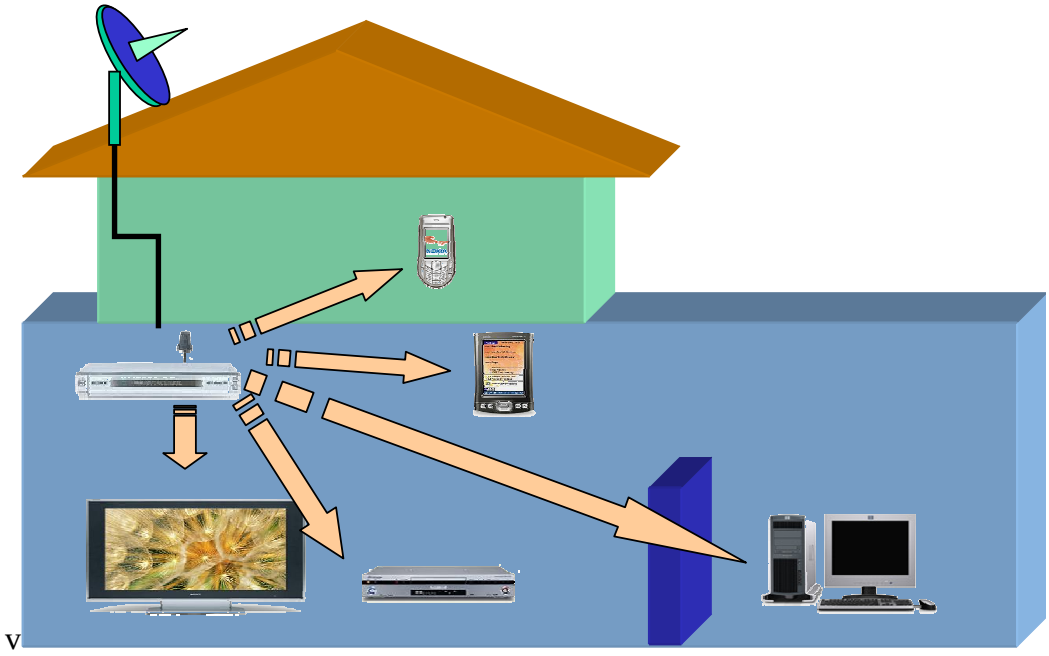

Fig. 2. A scenario demonstrates the multicast video service in residential environment.

Consider a real-time video stream that consists of α percent of BL and (1- α) percent of EL, where $1>\alpha>0$ and it can be estimated based on the type of video source or set by the video encoder. It is assumed that T_{max} (unit: Media Access Slot, MAS, which is 256 μsec in length and is the basic allocation time interval defined by MB-OFDM) is the maximum time reserved for the video for its real-time multicasting service; and B_{VI} (unit: bits) is the amount of video stream to be transmitted in a super-frame. Denote $SNR_{i,c}$ be the signal-to-noise-ratio (SNR) of the c-th user measured by the video server from the BP of the i-th super-frame. With the above mentioned information, we may select a proper modulation scheme for the EL. A robust modulation scheme requires more time to transmit EL packets but enables users with poor SNR

to decode the packets. Note that, the total transmission time required by BL and EL should be less than T_{max}. As mentioned, the SNR of the devices may be changed over time and thus, it leads to heavy computation complexity if we want to dynamically select the proper modulation scheme based on the up-to-date information of $SNR_{i,c}$. Due to the nature of the residential environment, the users may not change its location rapidly. Hence, it means that we may use the past information to reduce the required computation in selecting a new modulation scheme.

The coverage area within which a user can correctly decode a message transmitted by a given modulation scheme can be derived based on the SNR requirement of the modulation scheme and the path loss propagation model. Denote $M_{i,j}$ is the number of users in region j at super-frame I, where the region number is defined in Table 2. Note that $M_{i,j}$ can be estimated from the $SNR_{i,c}$ directly. Hence, the DRS aims to find the proper modulation scheme such that the average signal quality is maximized under the constraint of T_{max}. The DRS can be implemented based on a lattice diagram shown in Fig. 3. There are some decision thresholds that need to be computed. In each super-frame, the video server shall examine $M_{i,j}$ for j from 1 to 8. Details regarding to the updating of the thresholds and the decision algorithm can be referred to [6].

Region (j)	1	2	3	4	5	6	7	8
Maximum Attainable Transmission Rate ($R_{MAX,j}$)(Mbps)	480	400	320	200	160	106.7	80	53.3
Number of users in the j-th region	$M_{i,1}$	$M_{i,2}$	$M_{i,3}$	$M_{i,4}$	$M_{i,5}$	$M_{i,6}$	$M_{i,7}$	$M_{i,8}$

Table 2. $M_{i,j}$

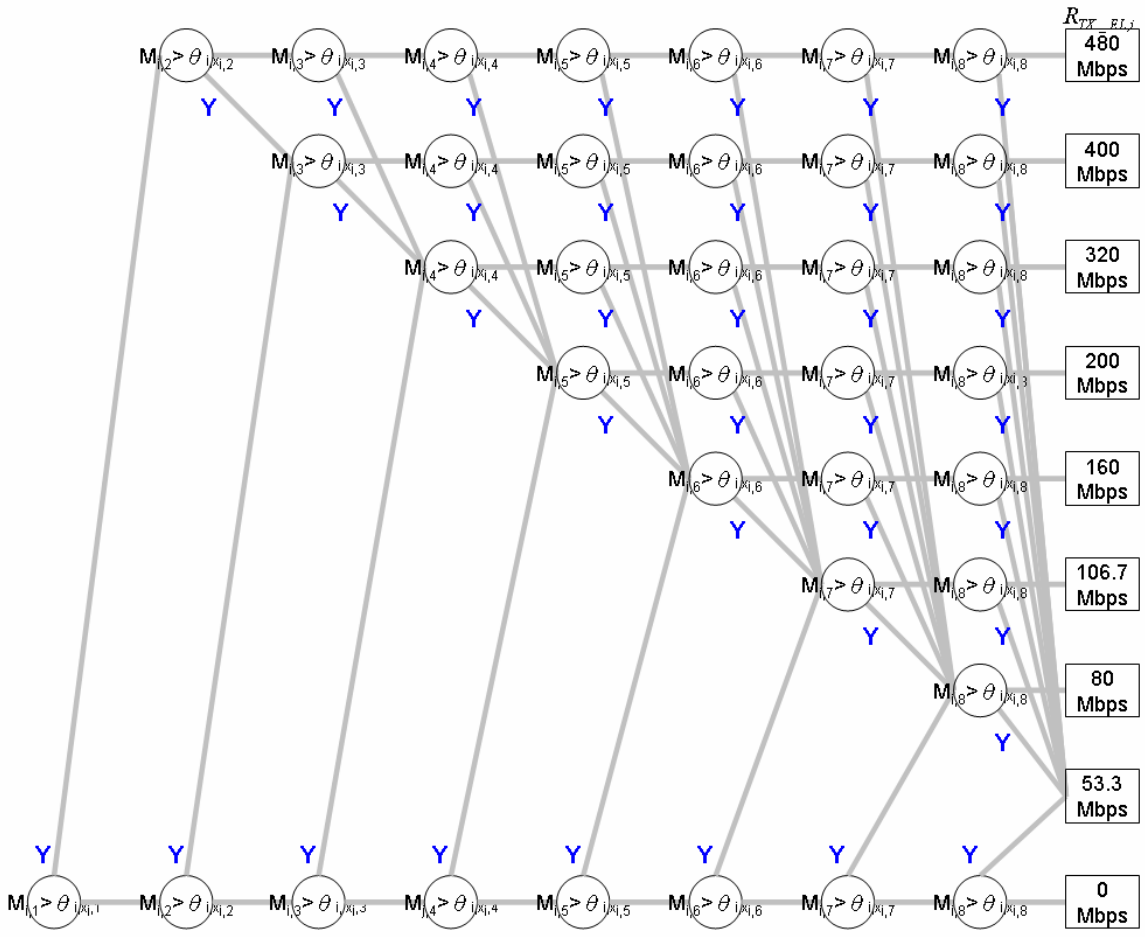

Fig. 3. A lattice diagram proposed for dynamic rate selection.

III. 效能討論

The performance of the proposed DRS is shown in Fig. 4. It can be shown that the proposed lattice diagram approach may significantly reduce the amount of computation up to 25% when the number of moving clients is large.

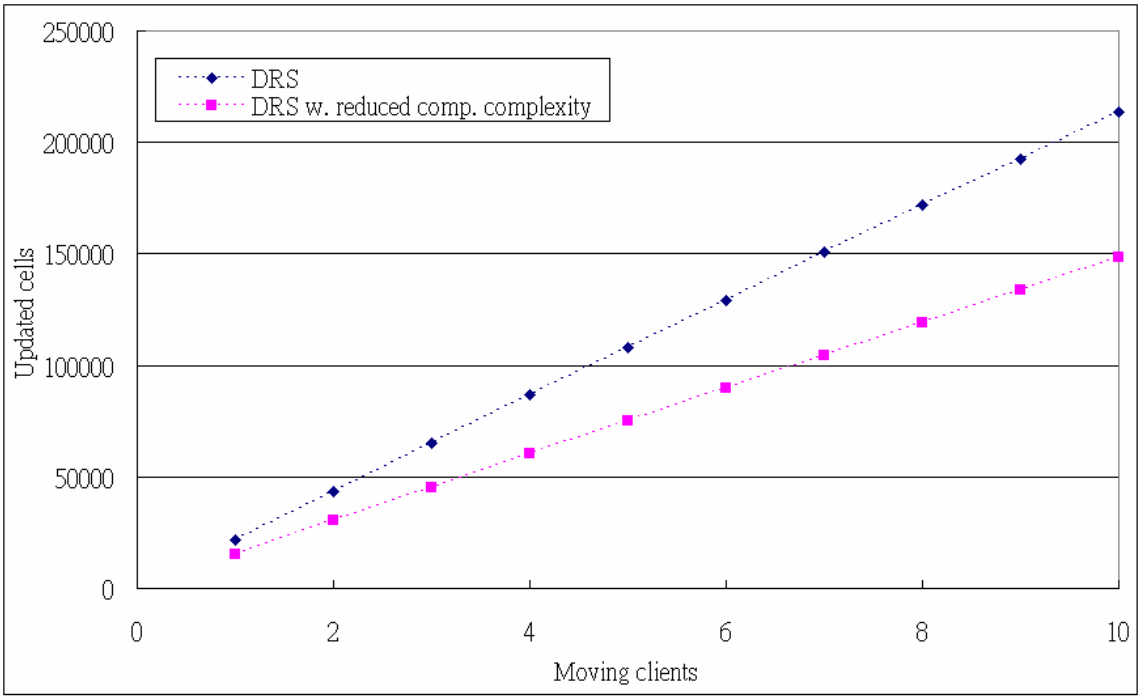

Fig. 4. The performance of DRS.

Cell radius	21.57028 m
Max. number of receivers	10
Location of the receiver	Uniformly distributed within the cell
Mobility model	random waypoint model with 8 directions
B_{VI}	10 Mbps x 65536 μs
α	0.7
Speed of the receiver	uniformly distributed between 0.5 to 1.5 m/s,

Table 3. Simulation parameters.

參考文獻

[1] Li-Hung Liao, Ray-Guang Cheng, and Kuo-Lun Hua, "Location-independent scheduling mechanism for multi-hop wireless backhaul networks," *IEEE VTC2007-Spring*, April 2006.

[2] Li-Hung Liao, Ray-Guang Cheng, and Kuo-Lun Hua, "Analysis of the virtual-timestamp-based scheduling for multi-hop wireless backhaul networks," *IEEE Wireless Communications and Networking Conference (WCNC)*, 2007

[3] Ray-Guang Cheng, Cun-Yi Wang, Li-Hung Liao, and Jen-Shun Yang, "*Ripple*: A wireless token-passing protocol for multi-hop wireless mesh networks," *IEEE Communications*

Letters, vol. 10, no. 2, pp. 123-125, Feb. 2006.

[4] Ray-Guang Cheng and Ruei-I Chang, "Improved wireless token ring protocol (IWTRP) for multi-hop wireless metropolitan area networks," *IEEE VTC2007-Spring*, April 2006.

[5] W. S. Conner, *et. al.*, "IEEE 802.11 TGs Usage Models," *IEEE P802.11-04/662r16*, Jan. 2005.

[6] Che-Sheng Lin, "支援超寬頻系統群播服務的動態速率選擇機制," Master Thesis, National Taiwan University of Science and Technology.

子計畫三、可重組式整合多模數位傳輸發展平台

I. 研究簡介

The Infrared Data Association (IrDA) defines physical specifications communication protocol standards for the short range transmission of data over infrared light. IrDA is a short-range optical communication technique and is often used to transfer data with the PC. It claims the cheapest to implement, the smallest in size, and the most power friendly wireless technology. It is also very secure due to the line-of-sight nature of infrared.

A standard called Very Fast Infrared (VFIr) was promoted by the IrDA for data rate of 16Mb/s [1]. UFIr (Ultra Fast Infrared) protocol that will provide up to 100 Mbit/s is also in development. Unfortunately, with the increase of data rate, the effect of component and channel induced inter-symbol interference (ISI) becomes more and more pronounced. To deal with such problem, VFIr adopts a modulation code HHH (1,13) code, which is a run length limited (RLL) code of coding rate R=2/3 and (d,k)=(1,13), to achieve the specified data rate [1]. We will explain the (d,k) constraint in the next section. This code overcomes the ISI problem by the d-constraint, which guarantees for at least d empty chips between chips containing pulses in the transmitted IR signal so that the decoder can compensate the ISI effect within two-chip width.

However, this approach fails for signals occupying more bandwidth. To enhance the robustness of indoor IR against ISI, one possible solution is to adopt RLL with stronger d-constraint. But increasing d will lead to much lower coding rate because we put more constraint on the selection of the codebook. Another approach is to introduce an equalizer in front of the decoder to compensate ISI effect. Examples of various equalizers can be found in many literatures [2][3]. In this report, we will focus on techniques combining equalization and decoding together in HHH-coded system.

II. 研究背景

A. RLL Sequences

Run length limited sequences [4] have played a key role for increasing the storage capacity of magnetic and optical disks or tapes. HHH (1,13) code used in VFIr is a kind of RLL sequence and is adopted in the IrDA specification. A (d, k) RLL sequence satisfies the following two conditions:

- d -constraint: two logical ”ones” are separated by a run of consecutive ”zeros” of length at least d.
- k-constraint: any run of consecutive ”zeros” is of length at most k.

B. Recommended Encoder/Decoder in IrDA-VFIr Mode

The encoding of the HHH (1,13) code is defined by a state transition table, which can be implemented as a set of encoding Boolean equations. First we define some signal vectors for the HHH encoder:

Data input:	$D = \{d_1, d_2\}$
Present (inner) state:	$S_{inner} = \{s_1, s_2, s_3\}$
Next (inner) state:	$N = \{n_1, n_2, n_3\}$
Internal data:	$\{B_1, B_2, B_3\}$
	$= \{\{b_1, b_2\}, \{b_3, b_4\}, \{b_5, b_6\}\}$
Codeword:	$C = \{c_1, c_2, c_3\}$

In every encoding cycle, these vectors are updated as follows:

$$B_1 \leftarrow B_2 \leftarrow B_3 \leftarrow D \quad (1)$$

$$S_{inner} \leftarrow N. \quad (2)$$

The components of *N* and *C* are computed by Boolean equations defined in [1]. Following the encoding rules defined in [1], one can notice that *N* and *C* are independent of *D*, and the data input *D* will affect the encoding output at next encoding cycle, according to (1).

For the HHH decoder, a simple decoder is provided in the appendix in [1], and it also can be described by some boolean equations.

III. Equalization for HHH-coded systems

In IrDA standard, HHH (1,13) code is introduced to compensate the ISI effect. This idea works only when the channel dispersion is limited within 2-chip duration; this approach will fail for higher data-rate requirements. However, HHH code is not only adopted to overcome the problem caused by ISI, but it also has good properties when considering issues such as power efficiency and clock synchronization [5]. Hence we keep the code structure and additionally introduce an equalizer to deal with ISI problems. Several types of equalizer can be found in literature. One of them is based on the maximum-likelihood sequence detection (MLSD) criterion [2], which yields optimal performance in ISI-channel with additive white Gaussian noise. ISI-channels are often described by FIR models. The input output relationship of such FIR channel can be represented by a finite-state machine (FSM). Then the Viterbi algorithm can be applied to find the optimal solution. For an FIR channel of *L* taps, the corresponding finite-state machine (FSM) has 2(*L*,1) states. We can take advantage of the *dk*-limitation of RLL codes to reduce the number of states on the trellis. For HHH (1, 13) code, not all of the $2^{(L-1)}$ states could happen. For example, for *L* = 7, there are only 21 possible states; the number of states is about 1=3 of that in the conventional Viterbi equalizer. The states having successive 1s never occur for HHH (1,13) code. Hence the number of states for a (*d, k*) RLL-coded system is equivalent to the number of *dk*-limited sequences (defined in 2.1) of length *n* = (*L*,1). It can be easily proved [4] that the number of possible states P_n, for a (*d, k*) RLL-coded system in an ISI channel of taps *L* = *n* + 1, can be calculated by:

$$P_n = \begin{cases} n+1, & 0 \le n \le d+1 \\ P_{n-1} + P_{n-d-1}, & d+1 \le n \le k \\ d+k+1-n+\sum_{i=d}^{k} P_{n-i-1}, & k < n \le d+k \\ \sum_{i=d}^{k} P_{n-i-1}, & n > d+k \end{cases}.$$

IV. Soft decoder

Since the encoding of the HHH (1,13) code is defined by a FSM, we can use a trellis to describe the encoding process, and then the Viterbi algorithm can be applied to achieve ML decoding performance.

HHH (1, 13) code can be represented as a 128-state time-invariant trellis code. For each state, we need 7 registers to record following information: inner-state {*s*1, *s*2, *s*3} and past input data bits {*b*1, *b*2, *b*3, *b*4}. Notice that, according to (1), the vector *B*3 = {*b*5, *b*6} is just the delayed version of the data input vector *D*. Hence we can treat *B*3 = {*b*5, *b*6} as the state input when describing the FSM structure, with one encoding cycle delay. In the following discussion, we call the 7-bit state {*s*3, *s*2, *s*1, *b*4, *b*3, *b*2, *b*1} an "outer-state" to make it distinguishable from the 3-bit "inner-state". The codeword {*c*1, *c*2, *c*3} and next inner state {*n*1, *n*2, *n*3} will only depend on the coming input bits and the outer-state.

V. Optimal joint equalization and decoding

Some works had proposed to perform equalization and decoding jointly. For joint MLSD (JMLSD), one can apply the Viterbi algorithm on the super trellis describing the cascade FSM of encoder and FIR channel. The number of states is upper bounded by the product of the states of the two FSMs. The super-state may be written as this form:

$$(\vec{c}_{past}, \{s_1, s_2, s_3\}, \{b_1, b_2, b_3, b_4\}),$$

where $\vec{c}_{past}$ denotes the past code-bits contributing ISI. Although we need to record additional past code-bits $\vec{c}_{past}$, we still can take advantage of the *dk*-constraint to reduce the number of states. For example, the past code-bit sequence $\vec{c}_{past}$ cannot have a subsequence with consecutive 1s so that we can cancel some illegal patterns. Similar method is also mentioned in [6] to form a combined trellis. The number of states may be further reduced in some ways [7], but this is behind the scope of this paper. We will take the performance of this optimal receiver as a baseline to compare the performance of other methods in the following discussion.

VI. Sub-optimal joint equalization and decoding

In the previous section, we had discussed the structure of JMLSD receiver. The performance of such a receiver is optimal; the remaining problem is the receiver complexity. The combination of code plus multi-path forms a "supercode" and the Viterbi algorithm needs to be operated on the corresponding "super-trellis", which leads to large complexity. Hence we seek for some algorithms having lower receiver complexity with only slight performance penalty. In this section, we provide some sub-optimal algorithms operating on the encoding trellis of the original HHH (1, 13) code.

A. Sub-optimal Algorithm I

The first proposed sub-optimal algorithm operates on the encoding trellis mentioned in section 4. The number of states is independent of the length of channel response even when ISI is considered. Basically we apply the conventional Viterbi algorithm [8] on this trellis, but each state/node additionally needs to record the ISI information causing from the past code-bits. Let $\vec{r}$ denote the received sequence and $\vec{v}(\vec{c})$ denote FIR-channel output sequence with input code

sequence $\vec{c} = (\vec{c}_0, \vec{c}_1, ..., \vec{c}_{N-1})$, which is of length 3*N* (since $\vec{c}_i = \{c_{i0}, c_{i1}, c_{i2}\}$). For optimal joint EQ and decoding, we are going to find a path $\vec{v}(\vec{c})$, where $\vec{c}$ is encoded from a information sequence $\vec{u}$, to minimize the Euclidean distance between $\vec{r}$ and $\vec{v}(\vec{c})$. The Euclidean distance is our metric and it can be written as

$$M[\vec{r}, \vec{v}(\vec{c})] = \sum_{i=0}^{N-1} ||\vec{r}_i - \vec{v}_i(\vec{c})||^2. \qquad (3)$$

We can express a partial path metric for the first *t* branches of a path as

$$M[\vec{r}, \vec{v}(\vec{c})]_{t-1} = \sum_{i=0}^{t-1} ||\vec{r}_i - \vec{v}_i(\vec{c})||^2. \qquad (4)$$

We denote the vector $\vec{v}_t(S_i, S_j)$ which begins from state *Si* and ends with state S_j, as a partial sequence of $\vec{v}(\vec{c})$. The vector $\vec{v}_t(S_i, S_j)$ is determined by current code-bits $\vec{c}_t = \{c_{t0}, c_{t1}, c_{t2}\}$ and past code-bits in previous stages $\vec{c}_{t-i}$, for *i* = 1,…,(*t*-1). We collect the contribution of past code-bits to $\vec{v}_t(S_i, S_j)$ into a newly defined ISI vector $\vec{p}_{t-1}(S_i)$. At the *t*-th stage, we define the ISI information vector (causing from the past code-bits and current codebits $\vec{c}_t$) $\vec{p}_t(S_i, S_j)$ from state S_i to state S_j by:

$$\vec{p}_t(S_i, S_j) = [p_0, p_1, \ldots, p_{(L-2)}]_{1\times(L-1)}. \qquad (5)$$

This vector $\vec{p}_t(S_i, S_j)$ is a function of $\vec{p}_{t-1}(S_i)$ and $\vec{v}_t$ and is calculated successively. At the beginning of transmission, $\vec{p}_{-1}(S_i, S_j)$ is a zero vector for all possible beginning state *Si*. There are several possible branches entering the state S_j, but only one of them can be the survivor. Among all possible branches entering the state S_j, if this branch (S_i, S_j) is the one with smallest partial metric, which is defined in equation (4), then we call this branch the survivor of state S_j, and the surviving ISI information vector, defined as $\vec{p}_t(S_j)$, is assigned by $\vec{p}_t(S_i, S_j)$. This vector $\vec{p}_t(S_j)$ is used to calculate $\vec{v}_{t+1}(\vec{c})$ of the next stage, and it may affect next several stages, depending on the level of channel dispersion. Since the newest code-bit in stage *t* is *ct*2 and this bit will cause ISI to next (*L*- 1) bits, the length of $\vec{p}_t(S_i, S_j)$ is (*L* -1).

Next we discuss the rule of calculating $\vec{v}_t(S_i, S_j)$ and $\vec{p}_t(S_i, S_j)$. Define the discrete time-variant channel response as $\vec{h} = [h_0 h_1, ..., h_{L-1}]$. Consider the branch from state S_i to S_j with branch output codeword $\vec{c}_t = \{c_{t0}, c_{t1}, c_{t2}\}$ at *t*-th stage and assume that the surviving ISI vector of state *Si* at stage (*t*-1) is

$$\vec{p}_{t-1}(S_i) = [I_0, I_1, \ldots, I_{L-2}]. \qquad (6)$$

The vector $\vec{v}_t(S_i, S_j)$ is determined by $\vec{c}_t = \{c_{t0}, c_{t1}, c_{t2}\}$ and the code-bits in the previous stage $\vec{c}_{t-i}$, for *i* = 1, …, (*t*-1). We have already collected the ISI contribution of past code-bits to $\vec{v}_t(S_i, S_j)$ into the surviving ISI vector $\vec{p}_{t-1}(S_i)$. Then $\vec{v}_t(S_i, S_j)$ can be computed by

$$\vec{v}_t(S_i, S_j) = \begin{bmatrix} c_{t0} \cdot h_0 + I_0 \\ c_{t1} \cdot h_0 + c_{t0} \cdot h_1 + I_1 \\ c_{t2} \cdot h_0 + c_{t1} \cdot h_1 + c_{t0} \cdot h_2 + I_2 \end{bmatrix}^T. \qquad (7)$$

The ISI information vector $\vec{p}_t(S_i, S_j)$ can be calculated by

$$\vec{p}_t(S_i, S_j) = \vec{q} + c_{t0} \cdot \vec{q}_0 + c_{t1} \cdot \vec{q}_1 + c_{t2} \cdot \vec{q}_2, \qquad (8)$$

where

$$\begin{array}{lcl} \vec{q} & = & [\ I_3, \ \ldots, \ I_{L-2}, \ 0, \ 0, \ 0\ ] \\ \vec{q}_0 & = & [\ h_3, \ \ldots, \ h_{L-2}, \ h_{L-1}, \ 0, \ 0\ ] \\ \vec{q}_1 & = & [\ h_2, \ \ldots, \ h_{L-3}, \ h_{L-2}, \ h_{L-1}, \ 0\ ] \\ \vec{q}_2 & = & [\ h_1, \ \ldots, \ h_{L-4}, \ h_{L-3}, \ h_{L-2}, \ h_{L-1}\ ] \end{array}.$$

The first term in equation (8), $\vec{q}$, is the ISI contribution due to past stages, and the rest is the contribution from current stage.

Here we summarize some key steps of our algorithm as follows:

1. At time $t = mT = 3mTc$ (where Tc is the bit duration), compute the partial metric for the single path entering each state.
2. Increase t by a time unit T. Compute the partial metric for all paths entering a state by adding the branch metric entering that state to the metric of the connecting survivor at the previous time unit. Additionally, compute the ISI information vector according to (8). For each state, compare the metrics of all possible paths entering that state, select the path with the smallest metric (the survivor), store it along with its metric and its ISI information vector, and then eliminate all other paths.
3. Repeat step 2 until reaching the end of the entire trellis.

B. *Dmin* Pattern

The minimum free distance *Dmin* of HHH (1, 13) code is 1. We define the *Dmin* pattern $\vec{e}$ as

$$\{\vec{e} = (\vec{u} - \vec{v}) | \min_{\vec{u},\vec{v}} w(\vec{u} - \vec{v}), \vec{u} \neq \vec{v}\}.$$

The function $w(.)$ returns the Hamming weight of the input sequence; vectors $\vec{u}$ and $\vec{v}$ are segments of codewords and they diverge from the same state S_i and then remerge with the same state S_j. Since *Dmin* = 1, the support of $\vec{e}$ contains only one element, defined by $\lambda(\vec{e})$. By computer search, we notice that for all possible $\vec{e}$ of length less than 15, the non-zero element never occurs in the first several code-bits. Table 1 lists all possible *Dmin* pattern ~*e* for partial codeword length $\leqq$ 15. In this table, the states S_i and S_j are of decimal representation converted from {*s*3*; s*2*; s*1*; b*4*; b*3*; b*2*; b*1}. We list one example for each possible *Dmin* pattern $\vec{e}$. It's interesting to note that $\lambda(\vec{e}) > 4$.

Let us examine why algorithm I is not optimal. Considering the codeword segment pair $(\vec{u}, \vec{v})$ with *Dmin*, the difference always happens at the tail part of $\vec{u}$ and $\vec{v}$. Once the nearby path is selected, incorrect ISI information will be passed to the next stage. This concept can be understood more clearly through figure 1. Two partial paths with $\vec{e}$ = [000000001] ($\lambda(\vec{e}) = 8$) are shown. The ISI information vector must be incorrect if an error path is selected since the code-bits at the remerging stage are different on these two paths. Oppositely, if $\vec{e}$ = [100000000], the ISI information can be preserved if the number of channel taps is less than 10. Here we define a new term, named by *tolerable zone* Z_T :

$$Z_T = \min_{\forall \vec{e}} [l(\vec{e}) - \lambda(\vec{e})] - 1, \qquad (9)$$

where $l(\vec{e})$ is the length of $\vec{e}$. This term stands for the largest tolerable zone that ISI can affect so that the past ISI information is still correct even if a nearby path is selected (a survivor) and other ISI information is eliminated. Then Z_T can be a good metric to judge if our sub-optimal algorithm is suitable or not for a certain code. Therefore, we will prefer a certain code that has *Dmin* pattern with large Z_T. However, HHH code does not meet our requirement because $Z_T = 0$.

(S_i, S_j); length	D_{min} pattern	(s_i, s_j); length	D_{min} pattern
(45,16); length = 9	000 001 000	(52,16) ; length = 15	000 000 000 100 000
(12,16) ; length = 9	000 000 100	(20,16) ; length = 15	000 000 000 010 000
(12,16) ; length = 9	000 000 001	(0,16) ; length = 15	000 000 000 001 000
(20,16) ; length = 12	000 000 000 100	(20,1) ; length = 15	000 000 000 000 100
(20,16) ; length = 12	000 000 000 010	(20,1) ; length = 15	000 000 000 000 010
(0,16) ; length = 12	000 000 000 001	(20,1) ; length = 15	000 000 000 000 001

Table 1. All possible D_{min} patterns with length ≤ 15.

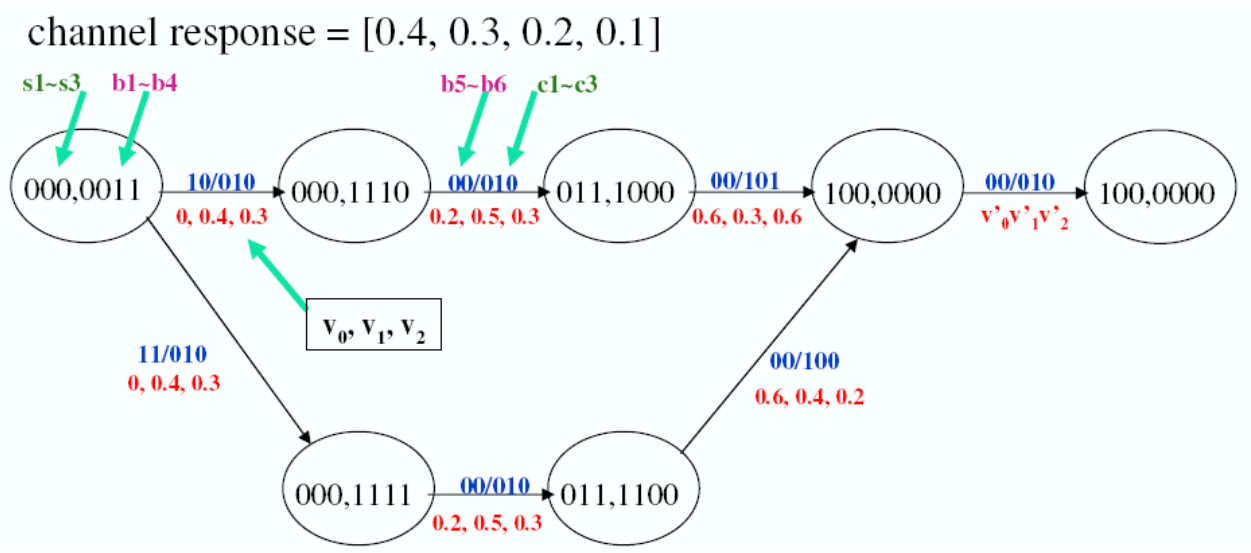

Fig. 1. An example to illustrate the concept of tolerable zone Z_T. In this case, $Z_T = 0$, and $\{v'_0, v'_1, v'_2\}$ may be determined improperly due to incorrect ISI information when an error path is selected.

C. Alternative System Structure and Sub-optimal Algorithm II

Instead of finding another coding technique with desired *Dmin* pattern to improve our sub-optimal algorithm, we propose another way to increase Z_T : transmit code-bits in reverse order. Then the tolerable zone Z_T can be raised to 5.

In this sub-section, we provide another system structure to improve the performance of our sub-optimal algorithm. The system block is depicted in figure 2. At the transmitting side, we add an LIFO (last in and first out) block after HHH encoder to reverse the order of transmitting

bitstream. Nevertheless, at the receiving side, we add an LIFO block after the joint decoder, instead of adding LIFO in front of the joint decoder. By doing so, the buffer size can be significantly reduced. The reverse-trellis joint decoder can be also implemented by the Viterbi algorithm, and the trellis is still the same as the original one. However, we decode from the end of the trellis. The partial metric of first *t* stages will be

$$M[\vec{r}, \vec{v}(\vec{c})]_t = \sum_{i=0}^{t-1} ||\vec{r}_i - \vec{v}_{(N-1-i)}(\vec{c})||^2. \qquad (10)$$

Thus, the first decoded information bit will be corresponding to the last transmitted information bit.

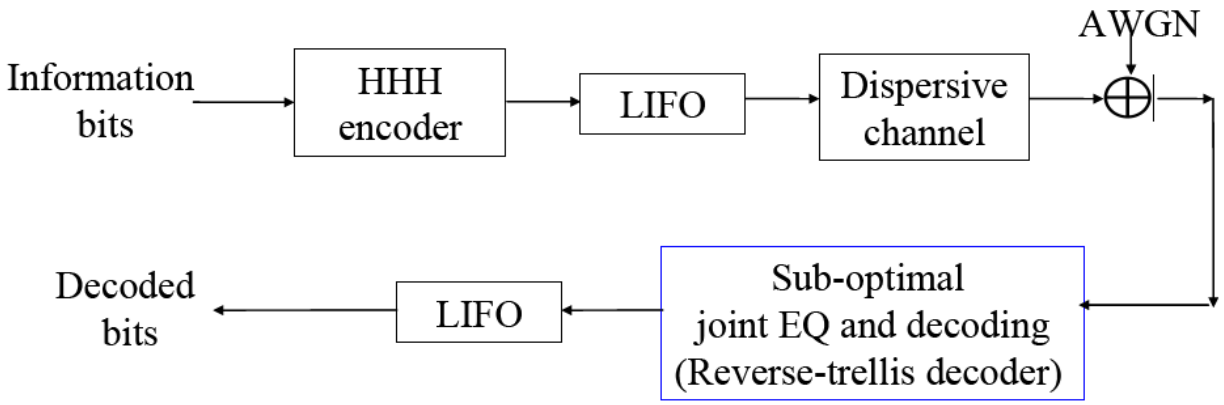

Fig. 2. Block diagram for sub-optimal algorithm II. LIFO is added to reverse the sequence order.

VII. Performance evaluation

A. Signal Model

Define the discrete time-variant channel response as $\vec{h} = [h_0 h_1, ..., h_{L-1}]$, where h_i's are real numbers. The input IR signals are $\vec{x} = [x_0, x_1, ..., x_n, ...]$, $x_i \in \{0,1\}$ and n is the time index. The received signal can be written as

$$y_n = \sum_{i=0}^{L-1} h_i x_{n-i} + w_n,$$

where w_n is modelled as white Gaussian noise. The input data x_i's are HHH encoded. The number of information bits per block is set to 1000 in our simulation. wo types of channel model will be examined:

² Type I, linear decay model: $h[n] = \kappa \cdot \sum_{i=0}^{L-1} (L-i) \cdot \delta[n-i]$ where κ is a normalizing factor so that $\sum_{i=0}^{L-1} h[n] = 1$.

² Type II, two-ray model: $h[n] = 0.5 \cdot \delta[n] + 0.5 \cdot \delta[n-\tau]$, where τ is a positive integer.

We define the electrical signal-to-noise ratio as $P^2 = R_b/N_0$ where P means the transmitted average power, R_b represents the information bit rate and N_0 represents the (two-sided) power spectral density of the white Gaussian noise.

B. Simulation Results

Here we evaluate the performance of various decoders in different multi-path environments. There are six decoders we are going to compare:

A. standard decoder recommended in IrDA-VFIr spec.

B. soft HHH (1; 13) decoder

C. a trellis equalizer followed by a standard decoder

D. joint EQ and decoding trellis decoder (Joint MLSD)

E. joint EQ and decoding with sub-optimal algorithm I

F. joint EQ and decoding with sub-optimal algorithm II.

First we compare the performance of decoder A and B in AWGN channel. In figure 3, we can observe that decoder B only improve the performance slightly (around 0.3 dB), since *Dmin* of HHH code is 1. For channel type I with $L = 4$, by comparing the performance of decoder E and F in figure 3, we can observe that the *reverse* operation does improve the performance of our sub-optimal algorithm. Also we can notice that decoder F can achieve the optimal performance

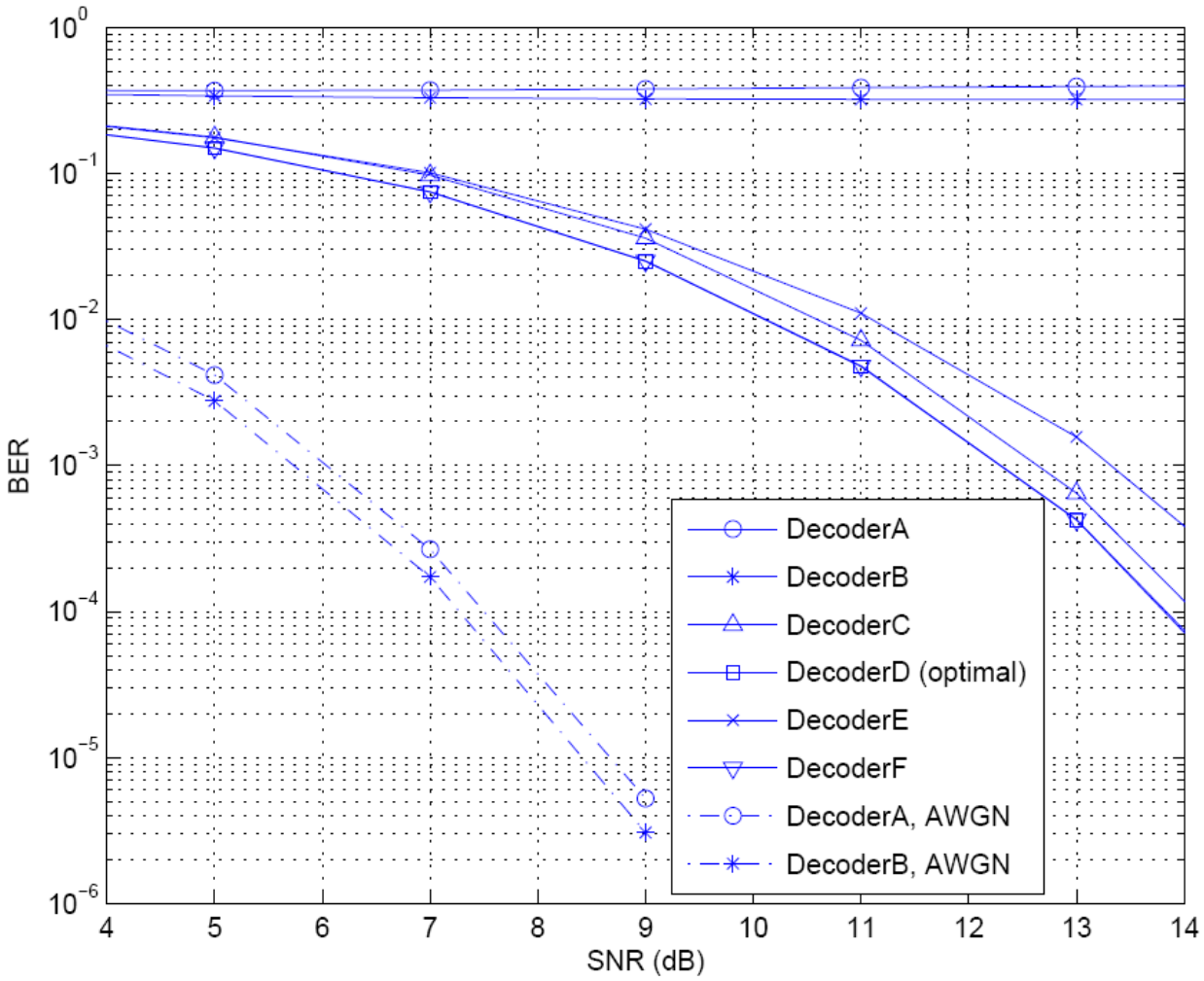

Fig. 3. BER in AWGN channel, and BER in channel type I with $L = 4$.

Also we give another simulation result based on channel type I with wider channel dispersion: $L = 8$ and $L = 10$. None of these two cases satisfy $Z_T \geqq (L\text{-}1)$. Figure 4 shows that even if $L > Z_T$, decoder F still outperforms decoder C about 0.25dB (at BER=10^{-4}), which is approximately equal to the performance gap between standard decoder (decoder A) and soft decoder (decoder B) in AWGN channel. Hence if the tail part of the channel response is not too

significant, our method still can yield good performance. In order to investigate the performance penalty of our sub-optimal approach resulted from wide channel dispersion, we further consider another channel model, type II. By varying τ, the position of the second path, we examine the performance if τ is larger than the tolerable zone Z_T. In figure 5, even if τ = 9, there is only 1dB SNR loss when comparing to decoder C at BER= 10^{-4}.

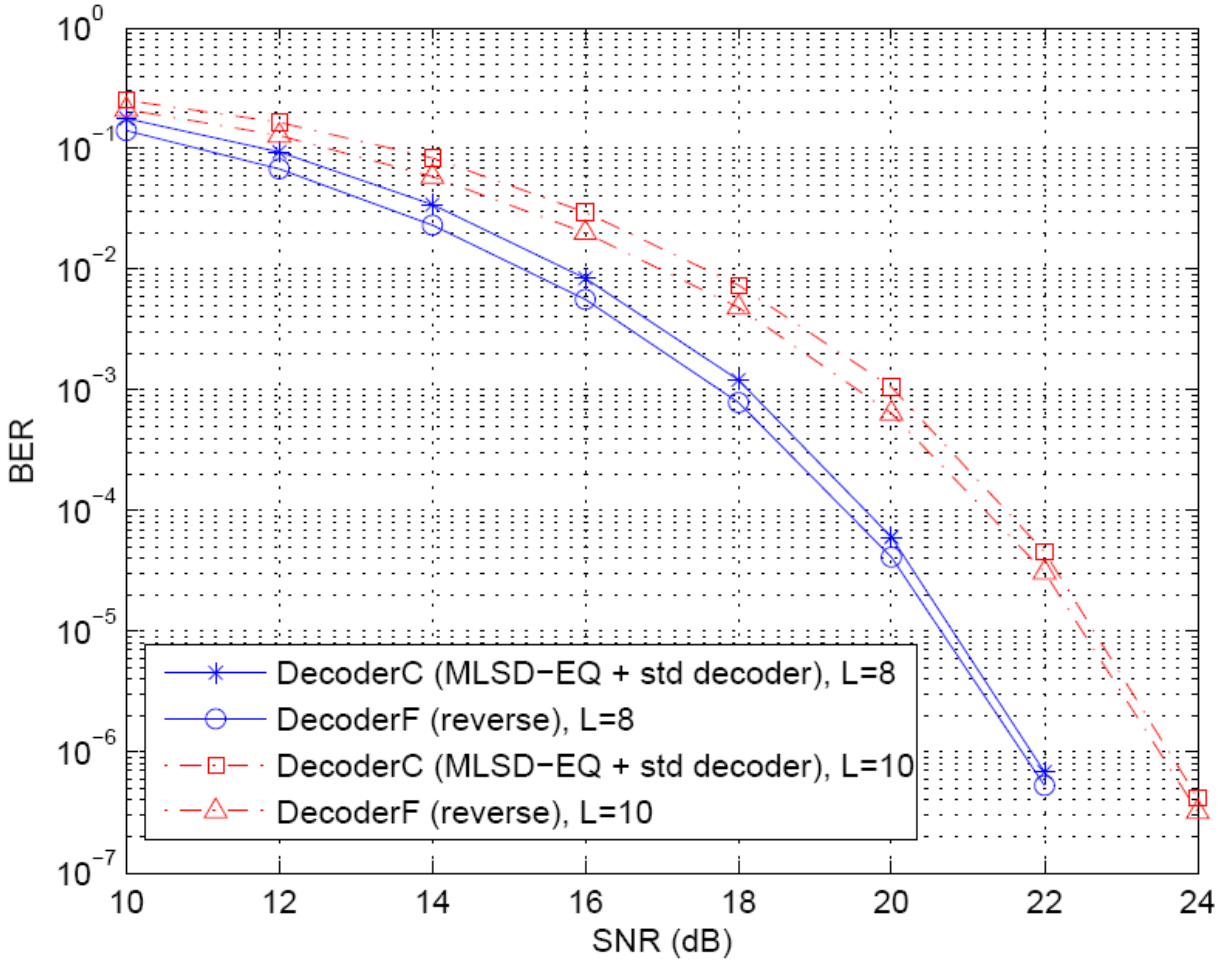

Fig. 4. BER for channel type I with L = 8; 10.

VIII. Conclusion

In this report, we have presented various methods to compensate ISI effects in the wireless infrared channel. Optimal equalizer for HHH-coded system is examined, and we take advantage of the properties of HHH code to reduce the complexity of this equalizer. For the design of combing equalization and decoding for HHH-coded system, we provide several approaches and evaluate their performance. JMLSD is an optimal approach to equalize and decode jointly; however, the computational complexity is quite high. Besides optimal joint receiver, we provide suboptimal approaches to combine equalization and decoding. The code design criterion of our sub-optimal algorithm is examined. Unfortunately, HHH (1, 13) code does not meet our requirement, but we give an alternative solution to come closer to the desired criterion. The simulation results show that our suboptimal approach still works well without redesigning the RLL code.

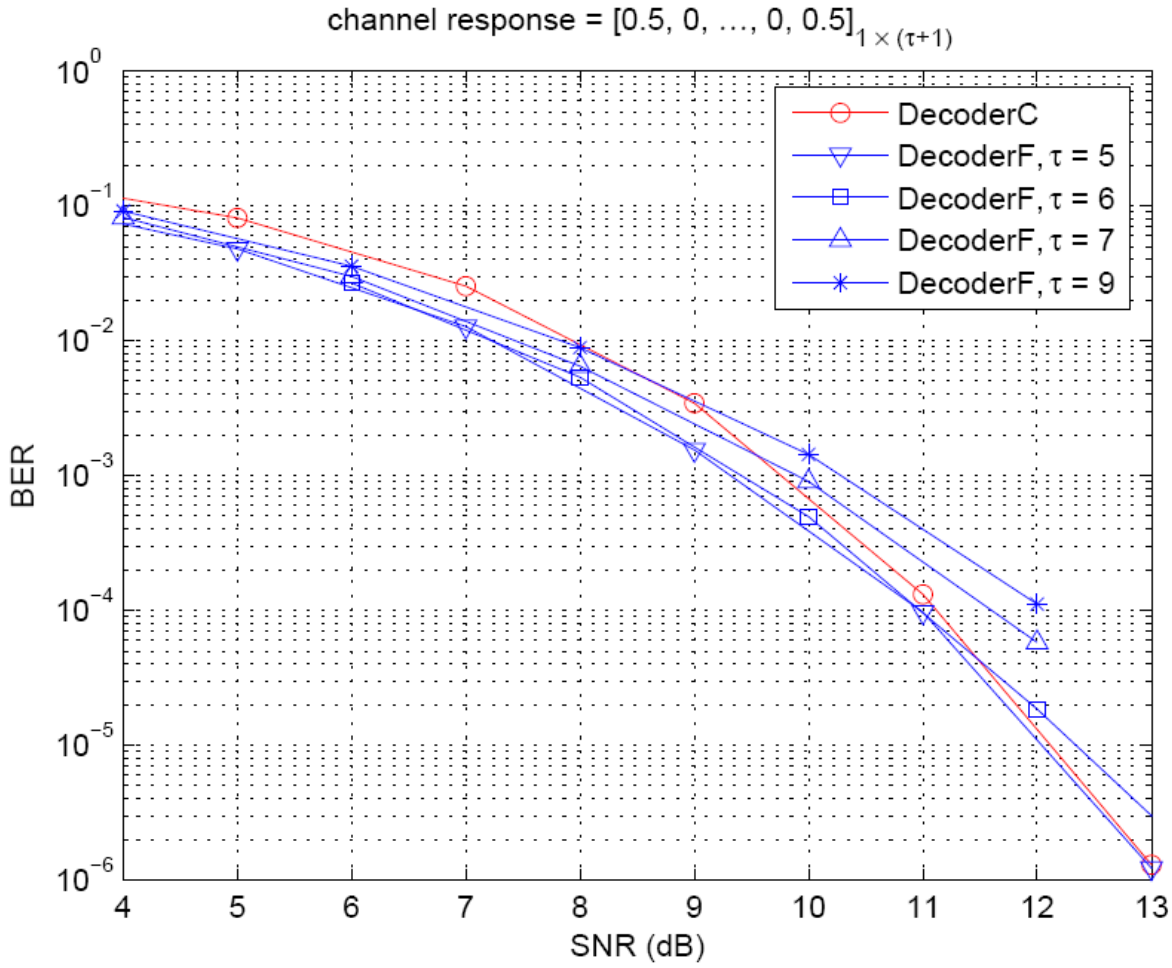

Fig. 5. BER for channel type II with different τ .

參考文獻

[1] *Infrared Data Association Serial Infrared Physical Layer Specification, v1.4,* Infrared Data Association, May 2001.

[2] G. D. Forney, "Maximum-likelihood sequence estimation of digital sequences in the presence of intersymbol interference," *IEEE Trans. Inform. Theory*, vol. 18, pp. 363–378, May 1972.

[3] John R. Barry, *Wireless Infrared Communications,* Kluwer Academic Publishers, 1994.

[4] Kees A. Schouhamer Immink, *Codes for Mass Data Storage Systems, second edition*, Shannon Foundation Publishers, 2004.

[5] W. Hirt, Z. M. Hassner, and N. Heise, "IrDA-VFIr (16 Mb/s): Modulation code and system design," *IEEE Personal Communication Magazine*, pp. 58–71, Feb. 2001.

[6] J. L. Fan, *Constrained coding and soft iterative decoding for storage*, Ph.D. thesis, Stanford Univ., Stanford, CA, 1999.

[7] Zhao Fang, G. Mathew, and B. Farhang-Boroujeny, "Joint turbo channel detection and RLL decoding for (1,7) coded partial response recording channels," in *Proceedings of IEEE ICC 2003*, May 2003.

[8] S. Lin and D. J. Costello, *Error control coding, second edition*, Prentice-Hall, 2004.

子計畫五、多標準共存之可調無線介接與正交分頻

I. 前言

This subproject is composed of five parts to discuss about five different issues.

Part I: Phase Noise Estimation in OFDM and OFDMA Uplink Communications
Part II: Characterizing the Wireless Ad Hoc Networks by Using The Distance Distributions
Part III: On the Distance Distributions of The Wireless Ad Hoc Networks
Part IV: Organizing an Optimal Cluster-Based Ad Hoc Network Architecture by the Modified Quine-McCluskey Algorithm
Part V: A Clustering Algorithm to Produce Power-Efficient Architecture for (N,B)-Connected Ad Hoc Networks

We discuss and present these five issues individually as follows.

Part I: Phase Noise Estimation in OFDM and OFDMA Uplink Communications

OFDM transmission technique has been adopted in several wireless communication standards for its capability of combating channel multipath fading with relatively low complexity while providing high spectral efficiency in comparison to single carrier transmission. An OFDMA system divides the available subcarriers into groups, called subchannels, and assigns one or multiple subchannels to multiple users for simultaneous transmission. OFDM is tremendously more sensitive to carrier frequency offset and phase noise than single carrier systems because the orthogonalities among OFDM subcarriers will be destroyed so that common phase error (CPE) and inter-carrier interference (ICI) will appear. OFDMA inherits from OFDM the weakness of being more sensitive to both of them than single carrier multiple access systems. Furthermore, because of the multiple phase noise of multiuser, phase noise will be more detrimental to uplink OFDMA systems if not carefully compensated

Part II: Characterizing the Wireless Ad Hoc Networks by Using The Distance Distributions

Wireless ad hoc network has been recognized as one of the possible solutions to realize the dream of pervasive computing especially when nodes are within the *dead zone*, an area where the exiting fixed infrastructures are unavailable, since nodes in the wireless ad hoc network can self-organize and operate without the help of the existing infrastructures. By using the multihop forwarding scheme, nodes in the wireless ad hoc networks exchange messages with other nodes that are not directly connected. However, due to the random deployment of the wireless ad hoc networks, the deployed network topologies are also random. As a result, some criterions are commonly used to characterize the random organized network.

Part III: On The Distance Distributions of The Wireless Ad Hoc Networks

Since nodes in wireless ad hoc networks may be randomly and independently spread over the

entire service area, the resulting network topologies are diverse and, thus, the separation distance between any selected node pair can be regarded as a random variable. Many characteristics of the wireless ad hoc networks are related to the separation distances between node pairs. One of the most important characteristics for the wireless ad hoc network to be applicable is the connectivity of the organized network. The most common approach to achieve the network connectivity is to maximize the transmission range so that nodes are connected. However, when the power consumption is considered, the transmission range should be optimized to the separation distance to its nearest neighbor.

Part IV: Organizing an Optimal Cluster-Based Ad Hoc Network Architecture by the Modified Quine-McCluskey Algorithm

When wireless nodes are in an area that is not covered by any existing infrastructure, one of the possible solutions to achieve the ubiquitous computing is to enable wireless nodes to operate in the ad hoc mode and self-organize themselves into a cluster-based network architecture. One of the general approaches to build up a cluster-based network architecture is to design an algorithm to organize wireless nodes into set of clusters. Within each cluster, a node is elected as a *clusterhead* (CH) to take responsible for the resource assignments and cluster maintenances. Many related algorithms have been proposed. The *minimum connected dominating set* (MCDS) approach tries to obtain an optimum configuration to be the virtual backbone of the wireless ad hoc networks. However, it is shown to be an NP-hard problem. The most feasible alternative is to find an approximated heuristic algorithm to obtain a sub minimum connected dominating set. The general idea among the related literatures is to select CHs based on some attributes of the networks.

Part V: A Clustering Algorithm to Produce Power-Efficient Architecture for (N,B)-Connected Ad Hoc Networks

Wireless ad hoc network is a self-organizing network that can be rapidly deployed and operated without the help of the existing infrastructure. Possible examples of the wireless ad hoc networks can be found in the tactical military applications, disaster recovery operations, exhibitions and conferences. Since there is no existing fixed infrastructure in the wireless ad hoc network, organizing the randomly deployed nodes into a virtual backbone turns out to be an important design issue. One of the general approaches is to organize nodes into groups of clusters. Within each cluster, a node is elected as the local controller of that cluster and is called clusterhead (CH). Major advantages of this approach include frequency spatial reuse, smaller interference and the increase of system capacity.

II. 研究目的

Part I: Phase Noise Estimation in OFDM and OFDMA Uplink Communications

Phase noise issue is an important topic in OFDM and OFDMA systems because it will destroy the orthogonalities among subcarriers. Models of phase noise source and the corresponding effects in OFDM systems are first introduced. There are various methods proposed to suppress

phase noise in OFDM systems. Here, we discuss a pilot-aided-decision-directed (PADD) approach for CPE estimation in OFDM systems. Conventional phase noise correction methods targeting at single phase noise, however, cannot be directly applied to uplink OFDMA transmissions because simultaneous transmitted user signals give rise to multiple phase noise. Extending from the PADD approach, two algorithms based on least-square and maximum likelihood criteria for estimation of Wiener phase noise in uplink OFDMA communications are discussed and compared.

Part II: Characterizing The Wireless Ad Hoc Networks by Using The Distance Distributions

Due to random deployment of the network nodes, the distances between nodes in the wireless ad hoc networks are random. Based on the developed distributions of the distance between nodes, the optimum transmission range to the *k*-th nearest neighbor, the most probable distance between two randomly selected nodes, the node degree and the network connectivity of the organized wireless ad hoc networks both in the ideal and shadow fading environments are characterized and evaluated. In addition, we also mathematically proof that the distribution of the node degree in the shadow fading environment is binomial. We apply the derived degree distribution to study the generalized *k*-connectivity problem of the wireless ad hoc network in the shadow fading environments.

Part III: On The Distance Distributions of The Wireless Ad Hoc Networks

Separation distance between nodes is an important index in characterizing the optimum transmission range, the most probable Euclidean distance between two random selected nodes, the node degree and the network connectivity of wireless ad hoc networks. However, because nodes are randomly deployed, the separation distances between nodes in the wireless ad hoc networks are also random. Thus, in this paper, we present methodologies to analyze three distance-related probability distributions: the distribution of the distance to the *k*-th nearest neighbor, the distribution of the distance between two random selected nodes and the joint distribution of the distances between nodes and a common reference node.

Part IV: Organizing an Optimal Cluster-Based Ad Hoc Network Architecture by the Modified Quine-McCluskey Algorithm

An optimal cluster-based ad hoc network architecture that requires the minimum number of cluster maintenance overheads not only reduces the waste of the precious bandwidth but also saves the consumption of the limited battery power. Mathematical analyses show that the cluster maintenance overheads can be minimized by minimizing the number of generated clusters and the variance of the number of cluster members. By using the Modified Quine-McCluskey (MQM) algorithm, the number of generated clusters and the variance of the number of cluster members of the generated cluster-based network architecture are minimized. Thus, the number of overheads required to maintain the cluster architecture is minimized and the precious bandwidth and the limited battery power are saved.

Part V: A Clustering Algorithm to Produce Power-Efficient Architecture for

(N,B)-Connected Ad Hoc Networks

Reducing the waste of the limited battery power in exchanging cluster maintenance messages is one of the important issues in designing clustering algorithm for the wireless ad hoc networks. Analyses show that this can be achieved by reducing the number of generated clusters and the variance of the number of cluster members. By assigning critical node (the only neighbor of boundary node) the highest weight (or priority) to be selected as a clusterhead, we show that the number of cluster maintenance overheads is reduced by the proposed Distributed Clustering Algorithm with Critical Node First (DCA/CNF) based approaches. As a consequence, the limited battery power is conserved and the organized network architecture is power efficient.

III. 研究方法

Part I: Phase Noise Estimation in OFDM and OFDMA Uplink Communications

OFDM transmission technique has been adopted in several wireless communication standards for its capability of combating channel multipath fading with relatively low complexity while providing high spectral efficiency in comparison to single carrier transmission. An OFDMA system divides the available subcarriers into groups, called subchannels, and assigns one or multiple subchannels to multiple users for simultaneous transmission. Signals from different users are overlapping in frequency domain but occupying different subcarriers, the orthogonality among subcarriers prevents multiple access interference (MAI) among users.

On the other hand, OFDM is tremendously more sensitive to carrier frequency offset and phase noise than single carrier systems [1] because the orthogonalities among OFDM subcarriers will be destroyed so that common phase error (CPE) and inter-carrier interference (ICI) will appear. OFDMA inherits from OFDM the weakness of being more sensitive to both of them than single carrier multiple access systems. Furthermore, because of the multiple phase noise of multiuser, phase noise will be more detrimental to uplink OFDMA systems if not carefully compensated [2].

Various methods to suppress phase noise in OFDM systems have been proposed in the literature [3]-[5]. However, they are specifically suitable for dealing with single phase noise. To mitigate multiple phase noise in OFDMA uplink, unavoidably, the adopted subcarrier assignment scheme needs to be taken into account since it affects the amount of MAI in the system. Two major subcarrier assignment schemes: subband-based and interleaved [6] are examined. The former divides the whole bandwidth into small continuous subbands, each user is assigned to one or several subbands. In the latter, subcarriers assigned to different users are interleaved over the whole bandwidth. An example of both schemes is illustrated in Fig. 1.

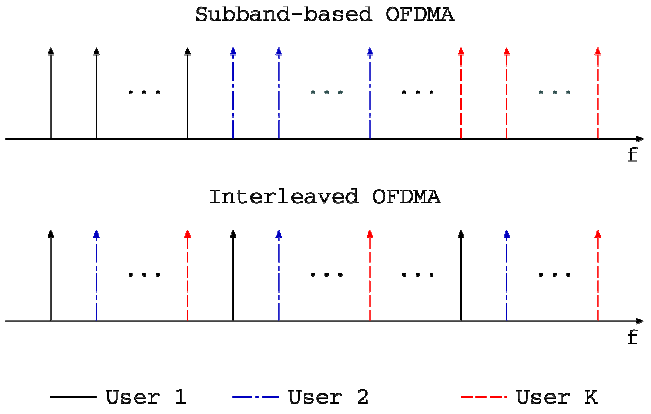

Fig. 1. Illustration of subband-based and interleaved subcarrier assignment schemes [16]

Part II: Characterizing The Wireless Ad Hoc Networks by Using The Distance Distributions

Wireless ad hoc network has been recognized as one of the possible solutions to realize the dream of pervasive computing 0-0 especially when nodes are within the *dead zone*, an area where the exiting fixed infrastructures are unavailable, since nodes in the wireless ad hoc network can self-organize and operate without the help of the existing infrastructures. By using the multihop forwarding scheme, nodes in the wireless ad hoc networks exchange messages with other nodes that are not directly connected. Possible examples of the wireless ad hoc networks are tactical military applications, disaster recovery operations, exhibitions or conferences. However, due to the random deployment of the wireless ad hoc networks, the deployed network topologies are also random. As a result, some criterions are commonly used to characterize the random organized network. In this part, we specifically focus on the following three criterions: the optimum transmission range to organize a wireless ad hoc network and the node degree and the connectivity of the organized network. Since the power of the nodes in the wireless ad hoc networks are mainly provided by the batteries, the optimum transmission range (or the critical transmission range) provides us how to power efficiently assign the transmission range either homogeneously or non-homogeneously so that the organized wireless ad hoc network is connected 0-0. The degree of a node is defined as the number of neighbors that are directly connected with 00 and is widely used as an index of the connectivity of the organized wireless ad hoc networks 0. The network connectivity is one of the most important criterions used to characterize the organized wireless ad hoc networks 0-00-0. This is mainly because for the multihop forwarding scheme in the wireless ad hoc network to be applicable there must exists at least one path between any two nodes so that the messages can be hop-by-hop forwarded to the intended destination nodes. When we look into the three criterions, we find that they are highly related to the distances between the nodes. For example, if the distances between node pairs in the deployed wireless ad hoc networks are short, smaller transmission power is enough for each node to reach its neighbors and, thus, the battery power is conserved. Furthermore, if the transmission range is fixed, shorter distances between nodes result in the higher node degree and the better connectivity of the deployed wireless ad hoc networks. However, due to nodes in the wireless ad hoc networks are in nature randomly and independently distributed into the service area, the distance between any node pair is also random. Thus, it is necessary to study the

stochastic property of the distances between nodes. Only few related researches are found in the literatures. In 0, by using two different distributions, uniform and Gaussian, to deploy nodes into the service area, Miller analyzed the distributions of the distance between two nodes in the wireless ad hoc networks and found that similar distance distributions are obtained by using different models to distribute nodes. Thus, he concluded that using a simple model to distribute nodes would be enough for the analysis and simulation of the wireless ad hoc networks. To obtain the joint distribution, Miller presented an alternative approach to find the marginal cdf of the distance between node and a randomly selected reference node (RN) 0. Then, by employing the independence property, the joint cdf of the distances between nodes and a RN was obtained.

Part III: On The Distance Distributions of The Wireless Ad Hoc Networks

Since nodes in wireless ad hoc networks may be randomly and independently spread over the entire service area, the resulting network topologies are diverse and, thus, the separation distance between any selected node pair can be regarded as a random variable. Many characteristics of the wireless ad hoc networks are related to the separation distances between node pairs. One of the most important characteristics for the wireless ad hoc network to be applicable is the connectivity of the organized network. The most common approach to achieve the network connectivity is to maximize the transmission range so that nodes are connected. However, when the power consumption is considered, the transmission range should be optimized to the separation distance to its nearest neighbor. Most of the connectivity related researches 0-0 are mainly based on the necessary condition that network is *k*-connected if the minimum node degree of a wireless ad hoc network is *k* 0. When the wireless ad hoc networks are operated in the ideal environment, the node degree can be easily obtained based on the pathloss model, i. e. the number of nodes within the predefined separation distances. However, in the shadow fading environment, given the separation distances between nodes and a common reference node (CRN), the node degree will dynamically change due to the random fluctuation of the signal strength. Thus, it is necessary to find the joint distance distribution between nodes and a CRN. In this part, we assume that nodes are uniformly and independently deployed within a square service area and the location of each random deployed node *u* is expressed as a vector $\mathbf{u} = (x_u, y_u)$ in $\mathbf{R}^2$. Based on the definition in 0, the *distance function* between nodes *u* and *v* is defined as $r(\mathbf{u}, \mathbf{v}) = ((x_v - x_u)^2 + (y_v - y_u)^2)^{1/2}$ such that (i) $r(\mathbf{u}, \mathbf{v}) \geq 0$, (ii) $r(\mathbf{u}, \mathbf{v}) = 0$ if and only if $\mathbf{u} = \mathbf{v}$, (iii) $r(\mathbf{u}, \mathbf{v}) = r(\mathbf{v}, \mathbf{u})$ and (iv) $r(\mathbf{u}, \mathbf{v}) \leq r(\mathbf{u}, \mathbf{w}) + r(\mathbf{w}, \mathbf{v})$ for any nodes *u*, *v* and *w*. In this case, the distance function is also known as the *Euclidean distance* between nodes *u* and *v* and the square service area is known as the 2-dimensional *Euclidean space*.

The first distance distribution we derived is based on the concept that if the Euclidean distance from a reference node to its *k*-th nearest neighbor is less than the transmission range of the reference node, the minimum degree of the node is *k*. The disadvantage of this distribution is that the prior knowledge of the order of the nearest neighbor of a reference node is required. To this end, we derive the distribution of the Euclidean distance between two random selected nodes without knowing the prior knowledge. Since the obtained results do not poss the independence property, they cannot be applied directly to obtain the joint distribution of the Euclidean distances between nodes and a common reference node. Therefore, we further derive the marginal cdf and pdf of the Euclidean distance between node and a common reference node.

Since the obtained marginal cdf and pdf possess the independence property, they can be easily generalized to obtain the joint cdf and pdf. Only few related researches are found in the literatures. The distribution of the *k*-th nearest neighbor is also known as Nearest Neighbor Distribution (NND) in 00. In 0, by using two different distributions, uniform and Gaussian, to distribute the nodes, Miller analyzed the distributions of the Euclidean distance between two nodes in the wireless ad hoc networks and noted that the models used to distribute nodes generate very similar cdfs. Thus, he concluded that using a simple model to distribute nodes would be enough for the analysis and simulation of wireless ad hoc networks. To obtain the joint distribution, Miller presented an alternative approach to find the marginal cdf of the Euclidean distance between two nodes 0. Then, by employing the independence property, the joint cdf of the Euclidean distances between node pairs that have a common reference node was obtained. In the following analyses, we assume the number of nodes in the network is *N* and ignore the boundary effects.

Part IV: Organizing an Optimal Cluster-Based Ad Hoc Network Architecture by the Modified Quine-McCluskey Algorithm

When wireless nodes are in an area that is not covered by any existing infrastructure, one of the possible solutions to achieve the ubiquitous computing is to enable wireless nodes to operate in the ad hoc mode [1] and self-organize themselves into a cluster-based network architecture. One of the general approaches to build up a cluster-based network architecture is to design an algorithm to organize wireless nodes into set of clusters. Within each cluster, a node is elected as a *clusterhead* (CH) to take responsible for the resource assignments and cluster maintenances. Many related algorithms have been proposed. The *minimum connected dominating set* (MCDS) approach [2] tries to obtain an optimum configuration to be the virtual backbone of the wireless ad hoc networks. However, it is shown to be an NP-hard [3] problem. The most feasible alternative is to find an approximated heuristic algorithm to obtain a sub minimum connected dominating set. The general idea among the related literatures is to select CHs based on some attributes of the networks. For example, the node degree, the link delay, the transmission power, the mobility, . . . , etc.. A detail survey of the clustering algorithms can be found in [4].

In viewing the previous works, we find that the minimization of the waste of the precious bandwidth and the limited battery power in exchanging the cluster maintenance overheads has not been well studied. Thus, based on the technique to select the optimum set of prime implicants in the Quine-McCluskey (QM) algorithm [5], we propose a Modified QM (MQM) clustering algorithm to organize the wireless ad hoc network into a cluster-based network architecture that requires the minimum number of cluster maintenance overheads.

Part V: A Clustering Algorithm to Produce Power-Efficient Architecture for (N,B)-Connected Ad Hoc Networks

Wireless ad hoc network is a self-organizing network that can be rapidly deployed and operated without the help of the existing infrastructure. Possible examples of the wireless ad hoc networks can be found in the tactical military applications, disaster recovery operations, exhibitions and conferences. Since there is no existing fixed infrastructure in the wireless ad hoc network, organizing the randomly deployed nodes into a virtual backbone turns out to be an

important design issue. One of the general approaches is to organize nodes into groups of clusters. Within each cluster, a node is elected as the local controller of that cluster and is called clusterhead (CH). Major advantages of this approach include frequency spatial reuse, smaller interference and the increase of system capacity.

Many related algorithms 0-0 have been proposed in the literatures. The minimum connected dominating set (MCDS) scheme 0 organizes the wireless ad hoc network into an optimum configuration. However, the problem to find the MCDS in a connected graph is shown to be NP-hard 0 and the problem to find the optimal CH set is an NP-complete problem 0. The general feasible alternative is to design an approximated heuristic algorithm to obtain a sub-optimal MCDS. The Degree-based clustering algorithms 0 are proposed to select CHs based on the degree of the nodes. The ID-based clustering algorithms 00 organize the cluster simply based on the node ID. Other approaches that are based on different node attributes can be found in 0-0. Due to the security concerns of the transmitted messages or the limitations of the geography of the service area, some singular nodes must/may be deployed within the service area. For example, some nodes in the networks have only one neighbor and are called boundary nodes. The only neighbors of boundary nodes play an important role in providing connections from boundary nodes to the other nodes. In view of the previous algorithms, we find that the impacts of the boundary nodes on the design of clustering algorithm have not been well studied in the literatures. This part addresses how to organize wireless ad hoc networks with boundary nodes into a power efficient cluster-based network architecture. The power efficiency of a cluster-based network architecture in this part is related to the number of overheads that are required to maintain the organized cluster-based network architecture.

Ⅳ. 結果與討論

Part I: Phase Noise Estimation in OFDM and OFDMA Uplink Communications

We can find the performance of these two CPE estimations by simulation. Consider an OFDMA system with 64 subcarriers in the 5 GHz frequency band. The signal bandwidth is 20 MHz. There are 4 sub-channels in the system, each contains 13 subcarriers. Each active user uses one sub-channel and the configuration and frequency domain structure of each subchannel are identical. We denote N_p the number of pilot subcarriers in a sub-channel and it varies from 1 to 4 in our experiments.

The channel response of each user is generated according the IEEE 802.11a channel model with root-mean-square delay spread equals to 50 ns. The channel coefficients are modeled as independent and complex-valued Gaussian random variables with zero-mean and an exponential power delay profile

$$\mathrm{E}\left\{\left|h_k(l)^2\right|\right\} = \lambda \cdot \exp\{-l\}, \qquad l = 0,1,\cdots,10.$$

The constant λ is chosen such that the signal power of each user is normalized to unity. The phase noise is generated by the Lorentzian model with β equals to 1 kHz. Two typical subcarrier assignment schemes: sub-band based subcarrier assignment and interleaved subcarrier

assignment as illustrated in Fig. 1 are used. Each simulation point is conducted using $3 \cdot 10^5$ frames, each frame consists of 16 OFDM symbols.

Fig. 1 shows the symbol error rate (SER) performance of the two proposed CPE estimators in comparison with both no-phase-noise and no-phase-noise-correction cases with QPSK. Since the number of pilot subcarriers affects the spectrum efficiency and the capacity of an OFDMA system, N_p is set to 1 in the simulation generating these two figures. Fig. 1(a) refers to sub-band based subcarrier assignment while Fig. 1(b) corresponds to interleaved subcarrier assignment.

First of all, the maximum likelihood (ML) approaches always have more improvement than least square (LS) ones, which is not surprising because the statistics of ICI term is taken into consideration. We can observe that when the number of active users increases, interleaved subcarrier assignment suffers more from the multiple-access interference because other active user's signals are at nearer subcarriers.

Fig. 2 illustrates how the performance of the proposed schemes changes with phase noise levels. The number of pilot symbols N_p is set to 1. The aim of the proposed schemes is to correct medium to small phase noise, i.e., for phase noise variance βT_s less than 10^{-4}. It shows in Fig. 7 that when phase noise variance is greater than 10^{-5}, the OFDMA system suffers remarkable performance degradation. However, the proposed CPE estimation schemes provide significant performance improvement over no-phase-noise-correction case.

When phase noise variance is less than 10^{-5} for an OFDMA system employing QPSK, we can see the error floor of the proposed schemes. For this phase noise variance range, it is not necessary to take the CPE correction to correct multiple phase noise.

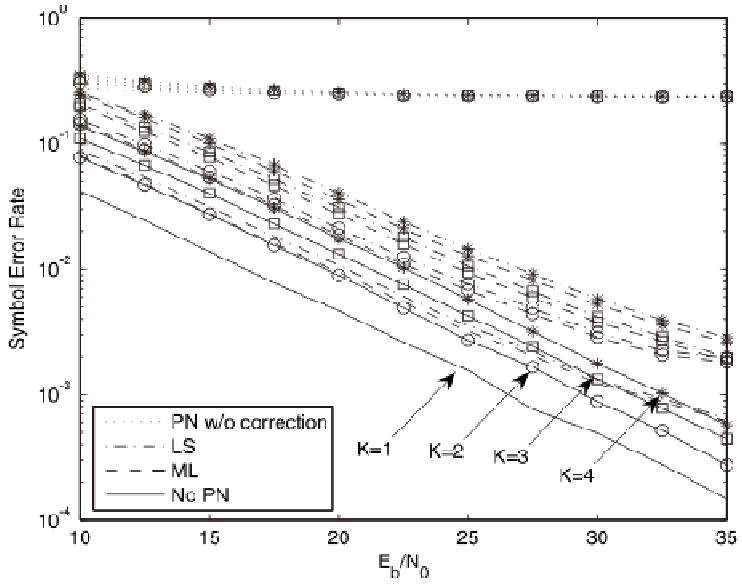

(a) Subband-based

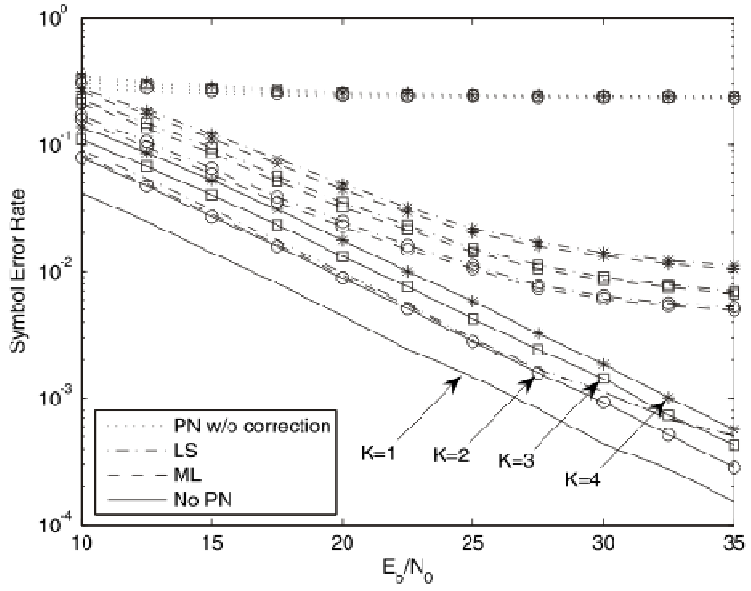

(b) Interleaved

Fig 1. Symbol error rate v.s. SNR with QPSK, K=1 to 4 [16]

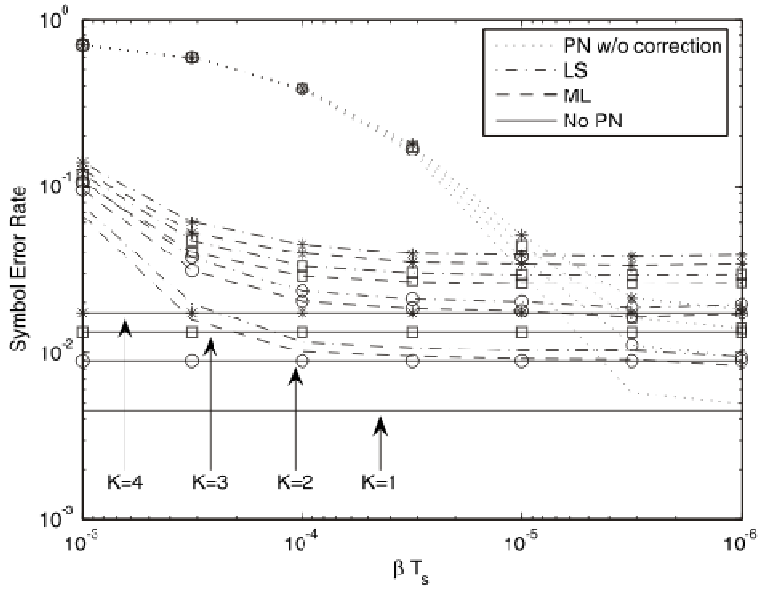

(a) Subband-based

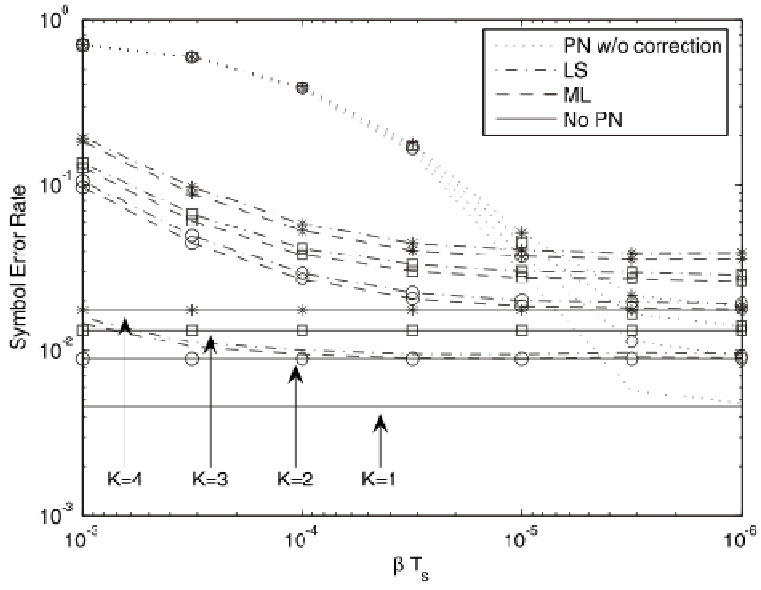

(b) Interleaved

Fig. 2. Symbol error rate v.s. phase noise variance with QPSK, K=1 to 4 [16]

Part II: Characterizing The Wireless Ad Hoc Networks by Using The Distance Distributions

Table 1 The Optimum Transmission Range for a 1-connected Wireless Ad Hoc Network

	p=0.95		p=0.99	
	N=100	N=200	N=100	N=200
r_1^{op}	155.33m	114.75m	171.22m	125.55m

Based on equation, the optimum transmission ranges to construct a 1-connected network r_1^{op} in a 1000m×1000m square-shaped service area with the probability $p = 0.95$ and $p = 0.99$, $N = 100$ and $N = 200$ are shown in Table 1. The probability of organizing a *k*-connected wireless ad hoc network in the ideal environment obtained in equation is shown in Fig. 1. This figure shows that the required transmission range *R* for *N* nodes in the ideal environment to organize a *k*-connected wireless ad hoc network is inverse proportional to *N* and proportional to *k*. For example, from TABLE 1 and Fig. 1, the transmission ranges 171.22m and 125.55m are required for a wireless ad hoc network with 100 and 200 nodes to be 1-connected with the probability 0.99. The probability of the wireless ad hoc network organized by *N* nodes in the shadow fading environment is *k*-connected as derived in equation is shown in Fig. 2. In this figure, the transmission range *R* is set to 300m which corresponds to a wireless ad hoc network organized by 100 nodes in the ideal environment is 3-connected with the probability greater than 0.9999 as shown in Fig. 1. With the same transmission range, Fig. 2 shows that as the channel variation is concerned, fewer nodes are required to achieve the same network connectivity and the number of nodes to achieve the required network connectivity is inverse proportional to the channel variation.

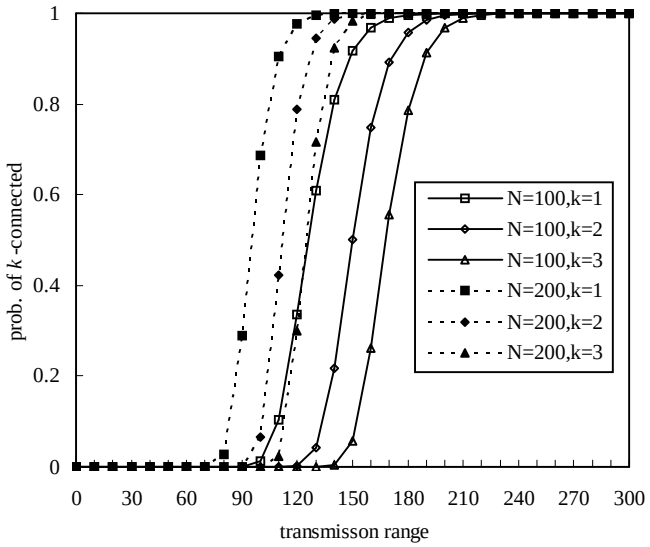

Fig. 1. The probability of *k*-connected in the ideal environment.

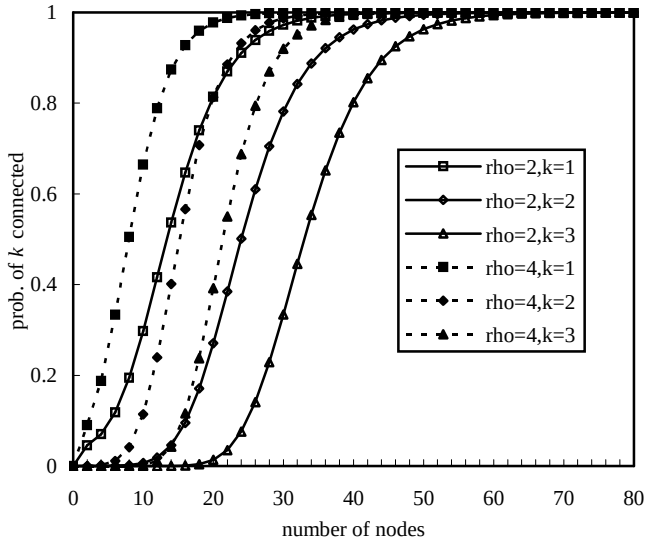

Fig. 2. The probability of *k*-connected in the shadow fading environment.

Part III: On The Distance Distributions of The Wireless Ad Hoc Networks

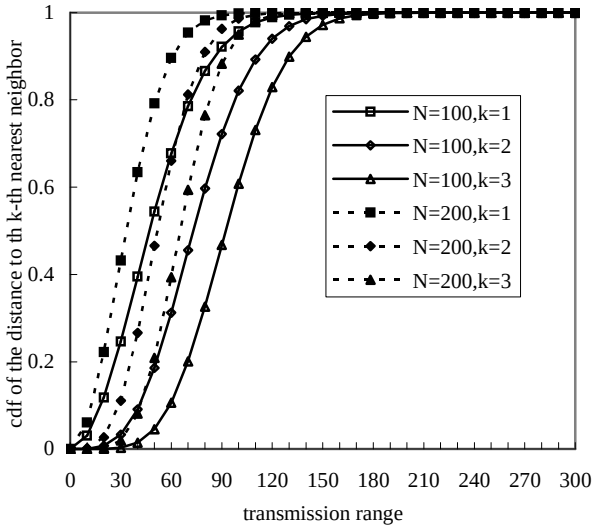

Fig. 1. The cdf of the distance to the *k*-th nearest neighbor.

The distribution of the distance to the k-th nearest neighbor

In Fig. 1, we show the cdf of the separation distance obtained in equation to the 1st, 2nd and 3rd nearest neighbor for a wireless ad hoc network with 100 and 200 nodes deployed over a 1000m× 1000m square-shaped service area. This figure shows that the distance to the *k*-th nearest neighbor is inverse proportional to the number of nodes in the service area. Furthermore, this figure also shows that almost surely that the first nearest neighbor is within the Euclidean distance 120m and 82m for the number of nodes are 100 and 200 respectively.

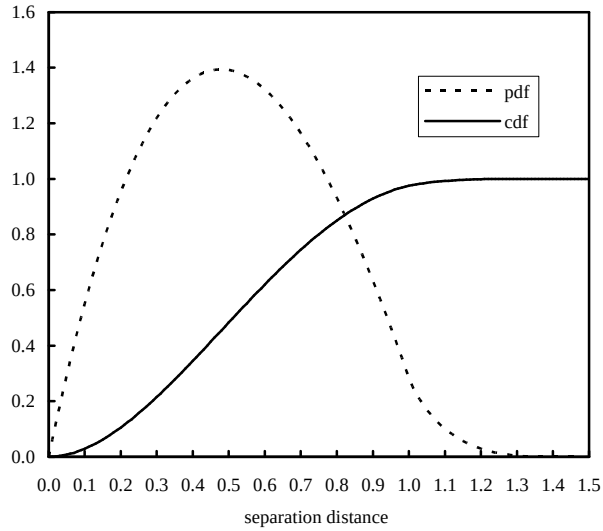

Fig. 2. The cdf and pdf of the Euclidean distance between two random selected nodes.

The distribution of the distance between two random selected nodes

The pdf and cdf in equations with different separation distance are shown in Fig. 2. By differentiating equation, the most probable normalized separation distance between two random selected nodes is 0.478. This can also be found from Fig. 2 that the 0.478 separation distance corresponds to the maximum probability density. Besides, from the cdf curve in Fig. 2, we find that if the normalized transmission range is higher than 0.94, the probability for two random selected nodes are connected is more than 0.95.

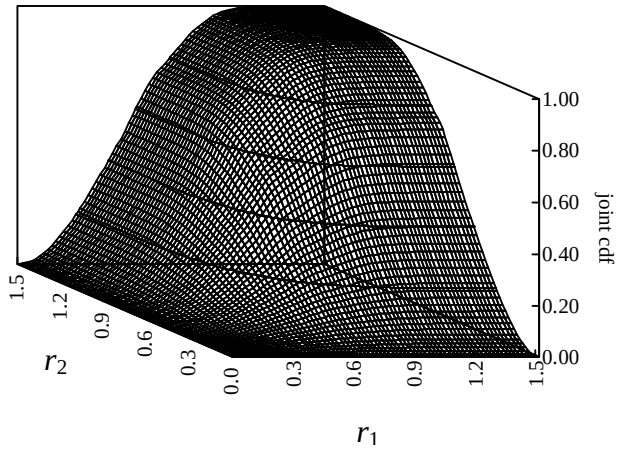

Fig. 3 The joint cdf of the distance $F_{shadow}(r_1, r_2)$.

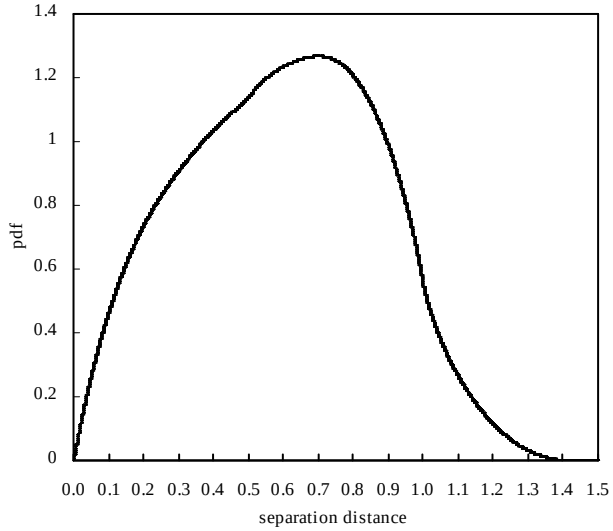

Fig. 4 The pdf of the distance between node and a CRN.

The distribution of the distance between node and a CRN

Based on equations, the conditional cdf of the separation distance in equation is obtained. By integrating equation, we can obtain the marginal cdf of the separation distance. Numerical integration of equation has been conducted for the joint cdf of the separation distances r1 and r2. The resulting joint cdf curve is shown in Fig. 3. Following the same procedures, the marginal pdf of the separation distance in equation is shown in Fig. 4. In this figure, the most probable normalized separation distance between node and a CRN is about 0.7.

Part IV: Organizing an Optimal Cluster-Based Ad Hoc Network Architecture by the Modified Quine-McCluskey Algorithm

We verify the performance of the proposed MQM algorithm by conducting extensive simulations. In our simulations, we assume the size of the service area is 2000m×2000m, the number of nodes *N* is 300 and the transmission range for each node is 300m. We run the simulation 10,000 times and average the collected data. In each simulation, we first randomly deploy the non-boundary nodes into a connected sub-network. Then, for each boundary node, a node in the connected subnetwork is randomly selected to be its only neighbor (i. e., the critical node). For the performance comparisons, the MQM and the Degree-based [6][7] clustering algorithms are used to cluster each of the generated network topology. As stated before, our objective is to design a clustering algorithm that can organize a cluster-based network architecture in which the required number of cluster maintenance overheads is minimized. In derived equation, the number of cluster maintenance overheads mainly depends on the number of generated clusters and the variance of the number of cluster members. The simulation results for the number of generated clusters and the variance of the number of cluster members are shown in Fig. 1 and Fig. 2 respectively. Since the original QM algorithm is designed to obtain the minimum set of PIs, the proposed MQM algorithm generates the minimum number of clusters as shown in Fig. 1. Furthermore, due to unchecked node is selected as a CH only if it is the critical node with the highest logical degree among its one-hop neighbors or it is the node with the highest logical degree among its two-hop neighbors, the number of clusters that are generated by the boundary node and the difference of the number of cluster members between clusters are

minimized. Therefore, as shown in Fig. 2, the variance of the number of cluster members is minimized. Consequently, the number of cluster maintenance overheads as shown in Fig. 3 is minimized and the generated cluster-based network architecture is optimal.

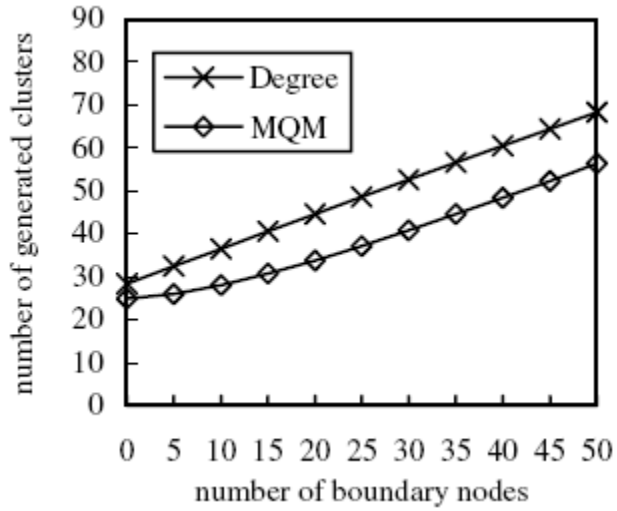

Fig. 1. The number of generated clusters

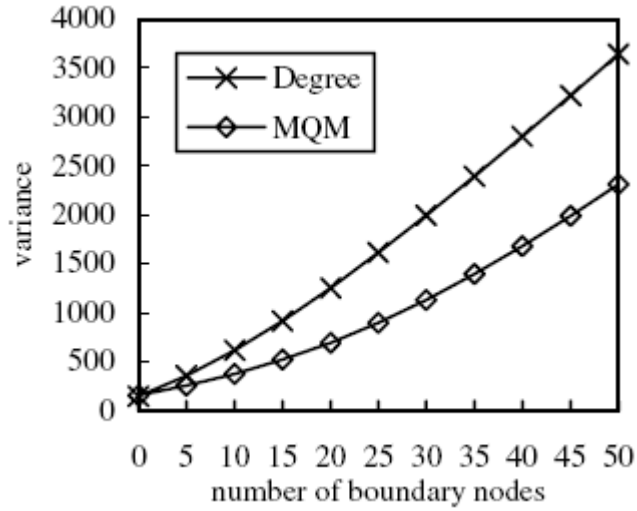

Fig. 2. The variance of the number of cluster members

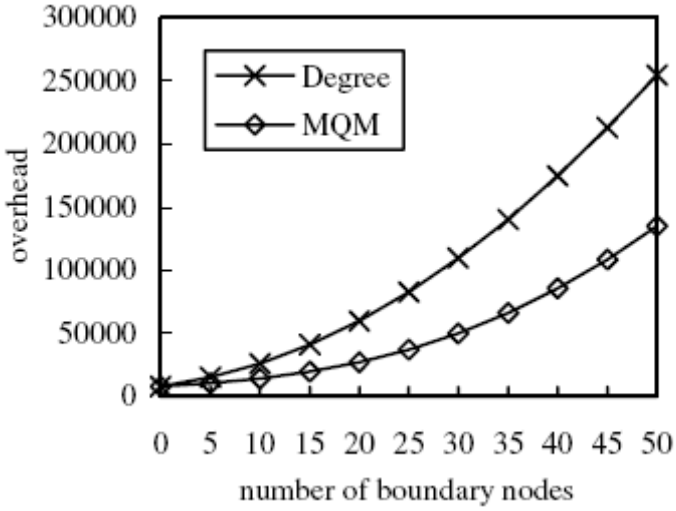

Fig. 3. The number of cluster maintenance overheads

Part V: A Clustering Algorithm to Produce Power-Efficient Architecture for (N,B)-Connected Ad Hoc Networks

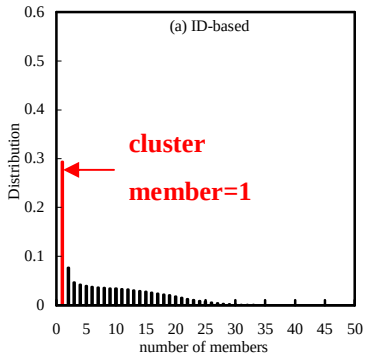

(a) ID-based clustering algorithms.

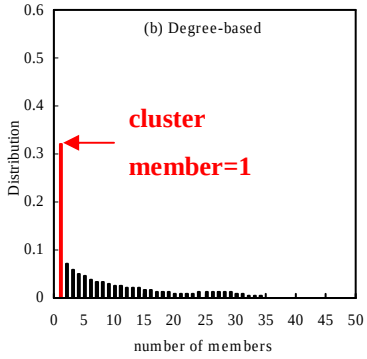

(b) Degree-based clustering algorithms.

Fig. 1. Distributions of the number of cluster members for clusters generated by (a) and (b)

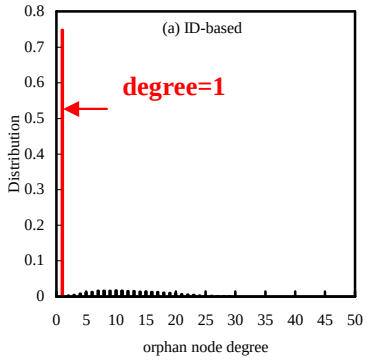

(a) ID-based clustering algorithms.

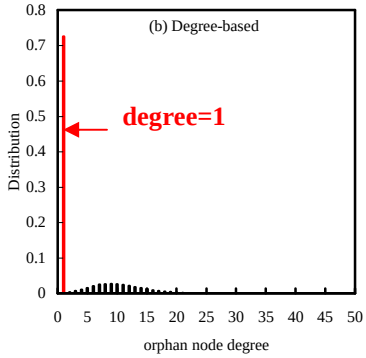

(b) Degree-based clustering algorithms.

Fig. 2. Degree distributions of the orphan nodes generated by (a) and (b)

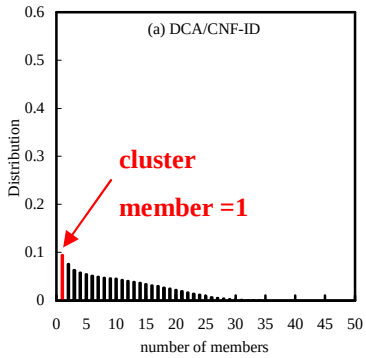

(a) DCA/CNF-ID clustering algorithms.

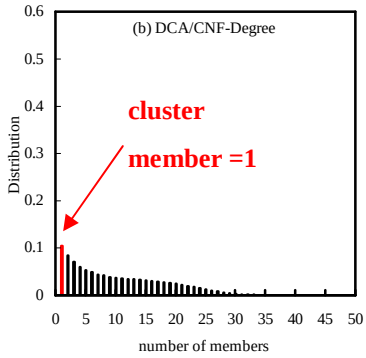

(b) DCA/CNF-Degree clustering algorithms.

Fig. 3. Distributions of the number of cluster members for (a) and (b)

We evaluate the performance of the DCA/CNF-ID and DCA/CNF-Degree approaches by conducting 10,000 simulations. We compare the simulation results with the ID-based and Degree-based algorithms. The service area is a 2000m×2000m square area. In each simulation, a (300,10)-connected wireless ad hoc network topology is randomly generated. Then, the ID-based, Degree-based, DCA/CNF-ID and DCA/CNF-Degree algorithms are used to organize the randomly generated network topology into a cluster-based network architecture. Fig. 3 shows the distributions of the number of the cluster members for the DCA/CNF-ID and DCA/CNF-Degree

approaches respectively. Comparing with the results as shown in Fig. 1, we can easily find that the number of orphan clusters generated by the proposed DCA/CNF-ID and DCA/CNF-Degree approaches is greatly reduced.

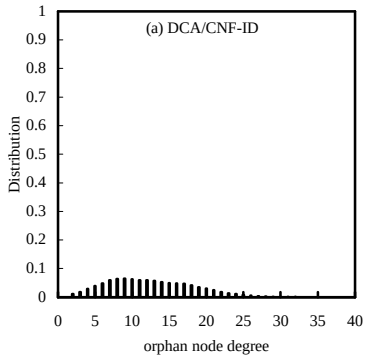

(a) DCA/CNF-ID clustering algorithms.

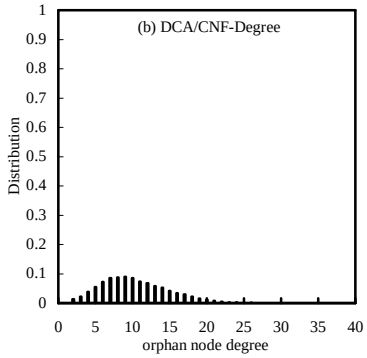

(b) DCA/CNF-Degree clustering algorithms.

Fig. 4. Degree distributions of orphan node generated by (a) and (b)

In Fig. 5, we show the distributions of the degree of the orphan node generated by the DCA/CNF-ID and DCA/CNF-Degree approaches respectively. Comparing with the results as shown in Fig. 2, no orphan nodes are boundary nodes!! In addition, we can also find that, with higher probability, the degree of the orphan nodes generated by the DCA/CNF-ID and DCA/CNF-Degree approaches is higher than that generated by the ID-based and Degree-based clustering algorithms. This is a good news since a higher degree of an orphan node implies that more chances for the orphan node to change into non orphan node either by joining a cluster organized by its one-hop neighbor or inviting its one-hop neighbors to join the cluster that it organizes when the cluster architecture is re-organized.

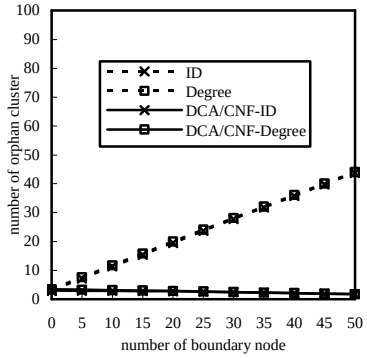

Fig. 5. The number of generated orphan clusters.

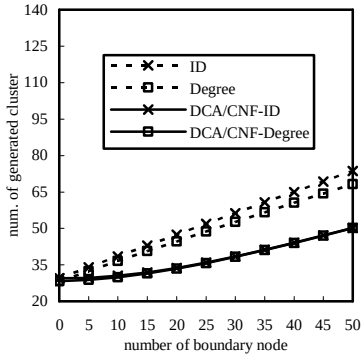

Fig. 6. The number of generated clusters.

The number of generated orphan clusters and the number of generated clusters are shown in Fig. 5 and Fig. 6 respectively. As stated in proposition , the number of generated orphan clusters in Fig. 5 is reduced by assigning critical node the highest weight in the proposed approaches. In Fig. 6, it is obviously that the number of generated clusters by the DCA/CNF-ID and DCA/CNF-Degree is reduced due to the reduction of the number of generated orphan clusters as stated in proposition.

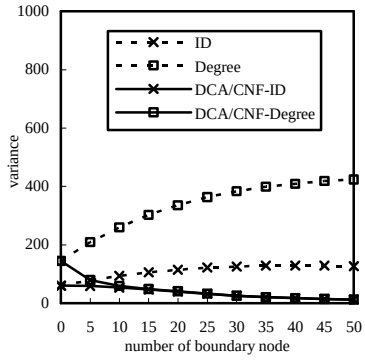

Fig. 7 The variance of the number of cluster members.

Fig. 7 shows the variance of the number of cluster members. As we mentioned before, due to the generated clusters are dominated by orphan clusters, the variance of the numbers of cluster members of the ID-based and Degree-based cluster algorithms are very high. On the contrary, due to the reduction of the number of generated orphan clusters, the proposed approaches reduce the variance of the number of cluster members. This figure also shows the Degree-based clustering algorithm is with the highest variance of the number of cluster members. This is because that CHs located in the dense area will have a larger number of cluster members than that located in the sparse area.

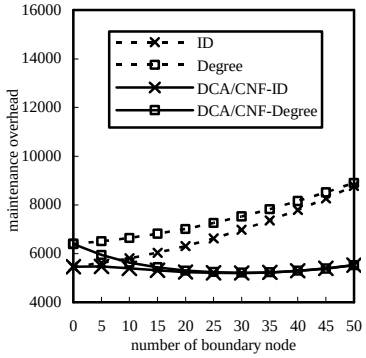

Fig. 8 The number of cluster maintenance overheads.

Fig. 8 shows the number of cluster maintenance overhead. Since the variance of the cluster members of the Degree-based clustering algorithm is much higher than the other three clustering algorithms as shown in Fig. 7, according to equation and Fig. 6, it has the maximum number of cluster maintenance overheads. By reducing the number of generated clusters and the variance of the cluster members, the number of cluster maintenance overheads for the proposed DCA/CNF based approaches is reduced. As a consequence, the limited battery power is conserved. Finally, from Fig. 5 to Fig. 8, we also observe that there is only little difference between results obtained by DCA/CNF-ID and DCA/CNF-Degree approaches. Based on this observation, we suggest that if the degree information of the neighboring nodes is not available or the node degree changes very frequently due to the mobility of the nodes or the dynamics of the channel quality, the DCA/CNF-ID approach is a good approach to organize the wireless ad hoc networks. However, if the degree information for neighboring nodes is available and the disadvantage of the biased CH election criterion to the lowest ID node is concerned, the DCA/CNF-Degree approach is a better approach to organize the wireless ad hoc networks.

Ⅴ. 成果與自評

Part I: Phase Noise Estimation in OFDM and OFDMA Uplink Communications

In this part, several phase noise models and the corresponding effects in OFDM and OFDMA systems are introduced. Among them, for the oscillator phase noise, we discussed the estimation of Wiener phase noise and stationary phase noise. Finally two multiuser phase noise estimation algorithms to mitigate the effects of multiple phase noise in uplink OFDMA systems are proposed. The LS approach provides acceptable performance with low complexity while the ML approach considers the second order statistics of the ICI to enhance the performance. The proposed schemes aim to compensate for CPE, the major effect of phase noise for medium to low phase noise levels where phase noise correction is applicable. Moreover, these two multiuser phase noise correction schemes are stable within a wide range of phase noise levels and applicable to any subcarrier assignment scheme, which shows its potential in practical applications.

Part II: Characterizing The Wireless Ad Hoc Networks by Using The Distance Distributions

To achieve pervasive computing in the absence of the existing infrastructure, nodes in the service area organize themselves into a wireless ad hoc network. Due to the random locations of the nodes, the distances between nodes are random. In this part, two distance distributions are presented and used as the foundations to characterize the organized wireless ad hoc networks. Given the prior knowledge of the order of the nearest neighbors, the nearest neighbor probability distribution in the theorem provides us how to use the optimum transmitting range to connect to the *k*-th nearest neighbor or, equivalently, how to power-efficiently deploy a *k*-connected wireless ad hoc network. Based on the marginal and the joint distribution of the distances between nodes and a RN in the theorem, we analytically show that the exact node degree of the wireless ad hoc network in the shadow fading environment is a binomial distribution. With the exact distribution of node degree, we further obtain the probability of the minimum node degree of the wireless ad hoc network that is the necessary condition of the network connectivity. Our results also show that the connectivity of the organized wireless ad hoc network in the shadow fading environment is improved due to the random fluctuation of signal strength.

Part III: On The Distance Distributions of The Wireless Ad Hoc Networks

This part investigates the probability distributions of the random separation distances between node pairs in the wireless ad hoc networks. By using the concept of the Euclidean distance in the 2-dimensional Euclidean space, the first probability distribution, the distribution of the Euclidean distance to the *k*-th nearest neighbor, is obtained. Using the technique of function of random variables, we obtain the probability distribution of the Euclidean distance between two random selected wireless nodes. Then, through the computation of the union area on the node coverage area and a unit square, we derived the marginal cdf and pdf of a wireless node pair. Since the Euclidean distances between wireless node pairs with the common reference wireless node are mutually independent, we can easily extend the marginal cdf and pdf to obtain the joint cdf and pdf of the Euclidean distances between wireless node pairs in the wireless ad hoc network with *N* wireless nodes that are randomly and uniformly distributed over a unit square.

Part IV: Organizing an Optimal Cluster-Based Ad Hoc Network Architecture by the Modified Quine-McCluskey Algorithm

To reduce the waste of precious bandwidth and the limited battery power in exchanging the cluster maintenance overheads, we propose a distributed Modified Quine-McCluskey (MQM) algorithm to organize the wireless ad hoc network into an optimal cluster-based network architecture that requires the minimum number of cluster maintenance overheads. Simulation results show that by minimizing the number of generated clusters and the variance of cluster members, the organized cluster-based network architecture requires the minimum number of cluster maintenance overheads. Thus, the optimal cluster-based network architecture is organized.

Part V: A Clustering Algorithm to Produce Power-Efficient Architecture for (N,B)-Connected Ad Hoc Networks

Through analyses, we find that reduction of the number of cluster maintenance overheads for a (*N*,*B*)-connected cluster-based wireless ad hoc network can be achieved by reducing the number of generated cluster and the variance of the number of the cluster members. By analyzing the cluster architectures generated by the ID-based and Degree-based clustering algorithms, we find that the number of generated cluster and the variance of the number cluster members can be reduced by reducing the number of orphan clusters generated by boundary nodes. Simulation results show that by assigning critical nodes the highest weights (or priorities) to be selected as CHs, the number of generated clusters and the variance of the number of cluster members for the cluster-based network architecture generated by the proposed DCA/CNF based approaches are reduced. As a consequence, the number of cluster maintenance overheads is reduced and the organized network architecture is power efficient.

參考文獻

Part I: Phase Noise Estimation in OFDM and OFDMA Uplink Communications

[1] T. Pollet, M. Van Bladel, and M. Moeneclaey, “BER sensitivity of OFDM systems to carrier frequency offset and wiener phase noise,” *IEEE Trans. Commun.*, vol. 43, pp. 191–193, Feb./March/April 1995.

[2] H. Steendam, M. Moeneclaey, and H. Sari, “The effect of carrier phase jitter on the performance of orthogonal frequency-division mutiple-access systems,” *IEEE Trans. on Comm.*, vol. 46, no. 4, pp. 456–459, Apr 1998.

[3] V. Abhayawardhana and I. Wassell, "Common phase error correction for OFDM in wireless communication," in *Proc. IEEE Global Telecommun. Conf (Globecom'02),* vol. 1, Taipei, ROC, Nov. 2002, pp. 17-21.

[4] S.Wu and Y. Bar-Ness, “A phase noise suppression algorithm for OFDM based WLANs,” *IEEE Commun. Lett.*, vol. 6, pp. 535–537, Dec. 2002.

[5] Y.-C. Liao and K.-C. Chen, “Estimation of wiener phase noise by the autocorrelation of the ici weighting function in ofdm systems,” in *Proc. Personal, Indoor and Mobile Radio Communications (PIMRC 2005)*, Berlin, Gremany, Sep 2005.

[6] Z. Cao, U. Tureli, and Y.-D. Yao, “Deterministic multiuser carrierfrequency offset estimation for interleaved ofdma uplink,” *IEEE Trans. on Comm.*, vol. 52, no. 9, pp. 1585–1594, Sep 2004.

[7] Yi-Hsueh Lin, “Phase Synchronization of Adaptive OFDM system,” Master thesis, Dept. of Communication Engineering Institute, National Taiwan University, Taipei, Taiwan, June 2003

[8] Elena Costa, Silvano Pupolin, “M-QAM-OFDM system performance in the presence of a nonlinear amplifier and phase noise”, *IEEE Trans. Comm.*, vol. 50, No.3, pp. 462-472, March 2002

[9] L. Piazzo and P. Mandarini, "Analysis of phase noise effects in ofdm modems," *IEEE Trans. on Comm.*, vol. 50, no. 10, pp. 1696-1705, Oct 2002.

[10] R. Van Nee and R. Prasad, *OFDM for Multimedia Wireless Communications*. Boston, MA:

Artech House, 2000.

[11] P. Robertson and S. Kaiser, “Analysis of the effects of phase noise in orthogonal frequency division multiplexing (OFDM) systems,” in *Proc. ICC’95*, pp. 1652–1657.

[12] B. Stantchev and G. Fettweis, “Time-variant distortion in OFDM,” *IEEE Commun. Letters*, vol. 4, no. 9, pp. 312-314, Sep 2000.

[13] Z. Jianhua, H. Rohling, and Z. Ping, “Analysis of ici cancellation scheme in OFDM systems with phase noise,” *IEEE Trans. on Broadcasting*, vol. 50, no. 2, pp. 97-106, Jun 2004.

[14] Yi-Ching Liao, “Carrier Synchronization of OFDM Systems over Dispersive Multipath Fading Channels,” Doctor thesis, Dept. of Communication Engineering Institute, National Taiwan University, Taipei, Taiwan, Oct. 2005

[15] S. He and M. Torkelson, “Effective SNR estimation in OFDM system simulation,” in *Proc. IEEE Global Telecommun. Conf. (Globecom'98)*, vol. 2, Nov. 1998, pp. 945-950.

[16] Y.-C. Liao and K.-C. Chen, “Multiuser Common Phase Error Estimation for Uplink OFDMA Communications,” in *IEEE Wireless Communications and Networking Conference (WCNC 2007)*, Mar. 2007.

[17] *Air Interface for Fixed Broadband Wireless Access Systems-Amendment 2: Medium Access Control Modifications and Additional Physical Layer Specifications for 2-11 GHz*, IEEE Std. 802.16a, 2003.

[18] P. H. Moose, “A technique for orthogonal frequency division multiplexing frequency offset correction,” *IEEE Trans. Commun.*, vol. 42, pp. 2908–2914, Oct. 1994.

[19] H. Sari, G. Karam, and I. Jeanclaude, “Channel equalization and carrier synchronization in OFDM systems,” in *Proc. 1993 Tirrenia Int. Workshop on Digital Communications 1993*.

[20] M. A. Visser and Y. Bar-Ness, “OFDM frequency offset correction using an adaptive decorrelator,” in *Proc. PIMRC’98*, pp. 816–820.

[21] M. A. Visser, P. Zong, and Y. Bar-Ness, “A novel method for blind frequency offset correction in OFDM systems,” in *Proc. CISS’32 1998*, pp. 483–488, Mar. 1998.

[22] M. S. El-Tanany, Y. Wu, and L. Hazy, “Analytical modeling and simulation of phase noise interference in OFDM-based digital television terrestrial broadcasting systems,” *IEEE Trans. Broadcast.*, vol. 47, pp. 20–31, Mar. 2001.

[23] R. A. Casas, S. L. Biracree, and A. E. Youtz, “Time domain phase noise correction for OFDM signals,” *IEEE Trans. Broadcast.*, vol. 48, pp. 230–236, Sep. 2002.

[24] S.Wu and Y. Bar-Ness, “A new phase noise mitigation method in OFDM systems with simultaneous CPE and ICI correction,” in *Proc. MCSS’03*.

[25] D. Petrovic, W. Rave, and G. Fettweis, “Phase noise suppression in OFDM including intercarrier interference,” in *Proc. International OFDM Workshop*, pp. 219–224.

[26] Songping Wu, Pan Liu, and Yeheskel Bar-Ness, “Phase Noise Estimation and Mitigation for OFDM Systems,” *IEEE Trans. on Wireless Comm.*, vol. 5, no. 12, Dec. 2006.

[27] K. Nikitopoulos and A. Polydoros, "Compensation schemes for phase noise and residual frequency offset in OFDM systems," in *Proc. IEEE Global Telecommun. Conf (Globecom'01)*, vol. 1, San Antonio, TX, Nov. 2001, pp. 25-29.

[28] T. Onizawa, M. Mizoguchi, T. Sakata, and M. Morikura, "A new simple adaptive phase tracking scheme employing phase noise estimation for OFDM signals," in *Proc. IEEE VTC'02 Spring*, vol. 3, Birmingham, AL, May 2002, pp. 1252-1256.

[29] S. He and M. Torkelson, “Effective SNR estimation in OFDM system simulation,” in *Proc. IEEE Global Telecommun. Conf. (Globecom’98),* vol. 2, Nov. 1998, pp. 945–950.

Part II: Characterizing The Wireless Ad Hoc Networks by Using The Distance Distributions

[1] Mark Weiser, “The computer for the 21st century.” Scientific American 265(3), 1991.

[2] J. Z. Sun, “Mobile ad hoc networking: An essential technology for pervasive computing,” Proc. of International Conferences on Info-tech & Info-net (ICII), vol.3, p.p. 316-321, 2001.

[3] M. Frodigh, P. Johansson and P. Larsson, “Wireless ad hoc networking: the art of networking without a network,” Ericsson Review, No.4, 2000, pp. 248-263.

[4] Y. C. Cheng and T. G. Robertazzi, “Critical connectivity phenomena in multihop radio networks,” *IEEE Trans. on Communications*, vol. 37, no. 7, pp. 770-777, 1989.

[5] P. Gupta and P. R. Kumar, “Critical power for asymptotic connectivity in wireless networks,” Stochastic Analysis, Control, Optimization and Applications: A Volume in Honor of W. H. Fleming, W. M. McEneany, G. Yin, and Q. Zhang (Eds.), Boston, MA: Birkhauser, 1998, pp. 547–566.

[6] C. Bettstetter, “On the connectivity of wireless multihop networks with homogeneous and inhomogeneous range assignment,” *IEEE VTC'02*.

[7] P. J. Wan and C. W. Yi, “Asymptotic critical transmission radius and critical neighbor number for k-connectivity in wireless ad hoc networks,” *ACM MobiHoc'04.*

[8] R. Hekmat and P. Van Mieghem, “Degree distribution and hopcount in wireless ad-hoc networks,” *IEEE ICON'03*.

[9] C. Bettstetter, “On the minimum node degree and connectivity of a wireless multihop network,” *ACM MobiHoc’02.*

[10] M. D. Penrose, “On k-connectivity for a geometric random graph,” Wiley Random Structures and Algorithms, vol. 15, no. 2, 1999, pp. 145-164.

[11] R. Hekmat and P. Van Mieghem, "Study of connectivity in wireless ad-hoc networks with an improved radio model," *WiOpt'04*.

[12] J. Ni and S. Chandler, “Connectivity properties of a random radio network,” *IEE Communications*, Vol. 141, pp.289-296, Aug. 1994.

[13] C. Bettstetter and C. Hartmann, “Connectivity of wireless multihop networks in a shadow fading environment,” *ACM MSWiM’03, 2003.*

[14] L. E. Miller, “Distribution of link distance in a wireless network,” *Journal of Research of National Institute of Standards and Technology*, vol. 106, pp. 401-412, March/April, 2001.

[15] L. E. Miller, “Joint distribution of link distances,” 2003 Conference on Information Sciences and Systems, The Johns Hopkins University, March 12–14, 2003.

[16] C. C. Tseng, H. T. Chen and K. C. Chen, “On the distance distributions of the wireless ad hoc networks,” *IEEE VTC 2006* Spring.

[17] D. B. West, Introduction to Graph Theory, Prentice Hall, 2001.

[18] T. Rappaport, Wireless Communications, Principles and Practice. Upper Saddle River Prentice-Hall PTR, 2002.

[19] B. Krishnamachari, S.B. Wicker, and R. Bejar, “Phase Transition Phenomena in Wireless Ad hoc Networks,” *IEEE GLOBECOM'01*.

Part III: On The Distance Distributions of The Wireless Ad Hoc Networks

[1] Y. C. Cheng and T. G. Robertazzi, "Critical connectivity phenomena in multihop radio networks," *IEEE Trans. on Communications*, vol. 37, no. 7, pp. 770-777, 1989.

[2] T. K. Philips, S. S. Panwar, and A. N. Tantawi, "Connectivity properties of a packet radio network model," IEEE Trans. on Information Theory, vol. 35, no. 5, pp. 1044-1047, 1989.

[3] P. Piret, "On the connectivity of radio network," *IEEE Trans. on Information Theory*, vol.37, no. 5, pp. 1490-1492, 1991.

[4] P. Santi and D. M. Blough, "An evaluation of connectivity in mobile wireless ad hoc networks," IEEE Proc. of the International Conference on Dependable System and Networks (DSN'02), 2002.

[5] P. Gupta and P. R. Kumar, "Critical power for asymptotic connectivity in wireless networks," in Stochastic Analysis, Control, Optimization and Applications: A Volume in Honor of W. H. Fleming, W.M. McEneany, G. Yin, and Q. Zhang, Eds. Boston, MA: Birkhauser, 1998, pp. 547–566.

[6] P. Panchapakesan and D. Manjunath, "On the transmission range in dense ad hoc radio networks," in *Proc. SPCOMM 2001*, Bangalore, India, July 2001, Paper 01-38.

[7] M. D. Penrose, "On k-connectivity for a geometric random graph," Wiley Random Structures and Algorithms, vol. 15, no. 2, 1999, pp. 145-164.

[8] S. K. Berberian, Fundamentals of Real Analysis, Springer, 1999.

[9] H. R. Thompson, "Distribution of distance to nth neighbor in a population of randomly distributed individuals," Ecology, vol. 37, no. 2, 1956.

[10] C. Bettstetter and C. Hartmann, "Connectivity of Wireless Multihop Networks in a Shadow Fading Environment," *ACM MSWiM'03, 2003.*

[11] L. E. Miller, "Distribution of link distance in a wireless network," Journal of Research of National Institute of Standards and Technology, vol. 106, pp. 401-412, March/April, 2001.

[12] L. E. Miller, "Joint distribution of link distances," 2003 Conference on Information Sciences and Systems, The Johns Hopkins University, March 12–14, 2003.

Part IV: Organizing an Optimal Cluster-Based Ad Hoc Network Architecture by the Modified Quine-McCluskey Algorithm

[1] M. Frodigh, P. Johansson and P. Larsson, "Wireless ad hoc networking: the art of networking without a network," Ericsson Review, no. 4, pp. 248-263, 2000.

[2] B. Das and V. Bhargavan, "Routing in ad-hoc networks using minimum connected dominating sets," in Proc. IEEE International Conference on Communications 1997, vol. 1, pp. 376-380.

[3] M. R. Garey and D. S. Johnson, Computers and Intractability: A Guide to The Theory of NP-Completeness. San Francisco: Freeman, 1978.

[4] J. Y. Yu and H. J. P. Chong, "A survey of clustering schemes for mobile ad hoc networks," IEEE Commun. Surveys and Tutorials, vol. 7, no. 1, pp. 32-48, first quarter 2005.

[5] E. J. McCluskey and H. Schorr, "Minimization of Boolean functions," Bell Syst. Tech. J., vol. 35, no. 5, pp. 1417-1444, Nov. 1956.

[6] R. Sivakumar, P. Sinha, and V. Bharghavan, "CEDAR: a core-extraction distributed ad hoc

routing algorithm," IEEE J. Sel. Areas Commun., vol. 17, no 8, pp. 1-12, Aug. 1999.

[7] M. Gerla and J. T. C. Tsai, "Multicluster, mobile, multimedia radio network," ACM/Baltzer J. Wireless Networks, vol. 1, no. 3, pp. 255-265, 1995.

Part V: A Clustering Algorithm to Produce Power-Efficient Architecture for (N,B)-Connected Ad Hoc Networks

[1] Das, B. and, Bhargavan, V., "Routing in ad-hoc networks using minimum connected dominating sets", IEEE International Conference on Communications (ICC), Vol. 1, pp.376-380, 1997.

[2] Greay, M. R. and Johnson, D. S., Computers and Intractability: A guide to the theory of NP-Completeness, Freeman, San Francisco, 1978.

[3] Li, C. S., "Clustering in packet radio networks", IEEE International Conference on Communications (ICC), pp. 283-287, 1985.

[4] Lian, J., Agnew, Gordon B., Nail, S., "A Variable Degree Based Clustering Algorithm for Networks", Proceedings of The 12th International Conference on Computer Communications and Networks, 2003, (ICCCN 2003), pp. 465-470.

[5] Lin, C. H., and Gerla, M., "Adaptive clustering for mobile wireless networks", IEEE Journal on Selected Area of Communications, Vol. 15, No. 7, pp. 1265-1275, 1997.

[6] Jiang, M. L., Li, J. Y. and Tay, Y. C., "Cluster based routing protocol (CBRP) functional specification", IETF Internet-Draft, 1998. http://www3.ietf.org/proceedings/98dec/slides/manet-cbrp-98dec/.

[7] Shah, M. J. and Flikkema, P. G., "Power-based leader selection in ad-hoc wireless networks", IEEE International Performance, Computing and Communications Conference (IPCCC), pp.134-139, 1999.

[8] Basu, P., Khan, N. and Little, Thomas D. C., "A mobility based metric for clustering in mobile ad hoc networks", IEEE International Conference on Distributed Computing Systems Workshop, pp. 413-418, 2001.

[9] Chatterjee, M., Das, S. K. and Turgut, D., "WCA: A Weighted Clustering Algorithm for Mobile Ad Hoc Networks", Journal of Cluster Computing (Special Issue on Mobile Ad hoc Networks), Vol. 5, No. 2, pp. 193-204, April 2002.

[10] Tseng, C. C. and Chen, K. C., "Power efficient topology control in wireless ad hoc networks", IEEE Wireless Communications and Networking Conference (WCNC), Vol. 1, pp. 610-615, 2004.

基於 802.16e 正交分頻多重存取系統之無線多媒體傳輸實現

Implementing Wireless Multimedia Transmission over OFDMA System Based on 802.16e

The Project of Consumer Networks

Cooperative Work

I. Introduction

This project focuses on the OFDMA system implementation on DSP board. The OFDMA system implementation and applications as video/audio transmissions or real-time multimedia transmissions are low-end and high-end goals in our project respectively.

Fig.1 shows the overall hardware structure. We utilize 1.TMS320C6416 DSP boards to build our OFDMA system (MAC and PHY included); 2.VDB daughter cards to obtain real-time compressed video from CCD camera, providing appropriate source coding for the our fixed-point signal processing; 3.Personal Computers to emulate channel with frequency selective fading. The connection between and PCs will be Ethernet.

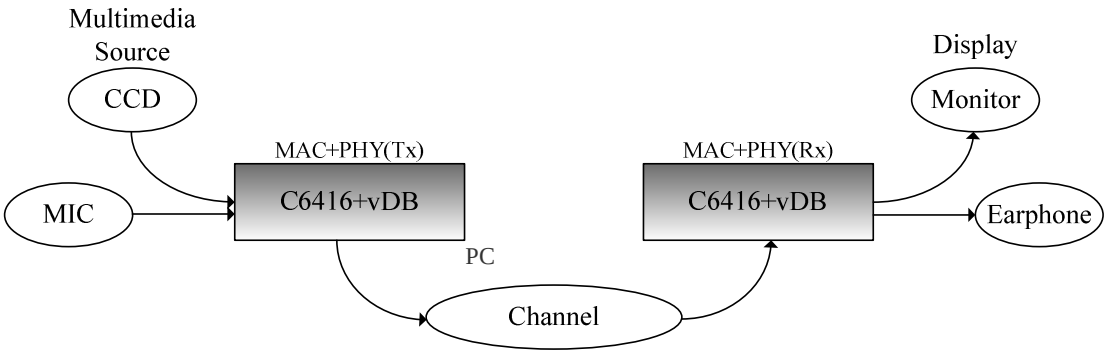

Fig.1 Hardware Structure

II. Functional Specification

We will build our OFDMA system on DSP boards including MAC and PHY layers. The corresponding functions are listed as below:

MAC layer	PHY layer
Guaranteed QoS for high-end use	FEC codes
Making up MPDU format	PSK modulation
Packing	OFDMA modulator
Fragmenting	Timing
Scheduling	Frequency offset synchronization

Table.1 MAC and PHY functions

III. Technique Specification

A. Medium Access Control (MAC) Layer

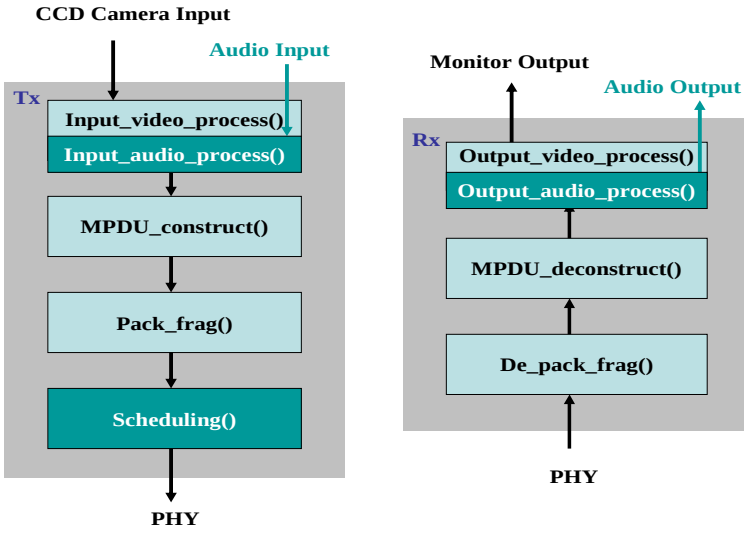

Fig. 2 MAC layer structure

Fig. 2 shows the overall structure of MAC layer we will build in our OFDMA system. Video/Audio signals will enter DSP board from MIC or CCD camera, and then the data will be sent to MAC layer. The main function of MAC is to construct the MAC PDU. After packing, fragmentation and scheduling, the data packet will then be sent to PHY for transmission. The detailed functions are described as follows:

1. *Function in C:* ***MPDU_construct()*** *and* ***MPDU_deconstruct()***

   Description: When data was received from upper layer, the main function of MAC I s to construct the MAC PDU. Compare to standard, we will use shorten header (1 byte) and remove CRC to avoid overhead.

2. *Function in C:* ***Pack_frag()*** *and* ***De_pack_frag()***

   Description: Fragmentation is the process by which a MAC SDU is divided into one or more MAC PDUs. In order to improve the transmitting efficiency, the MAC may pack multiple MAC SDUs into single MAC PDU. We will use fixed-length packing.

B. Physical (PHY) layer

I. Transmitter

OFDMA transmitter structure is basically the same as that of traditional OFDM transmitter. Besides, the parts of ***forward error correction (FEC)*** and ***bit-interleaver*** are added in the block diagram as high end blocks. High-end block means that it will function in the high-end implementation. As the characteristic of OFDMA technique, one user using some set of sub-carriers, the block of sub-carrier allocation is adopted here. The overall structure of OFDMA transmitter is shown in Fig. 3.

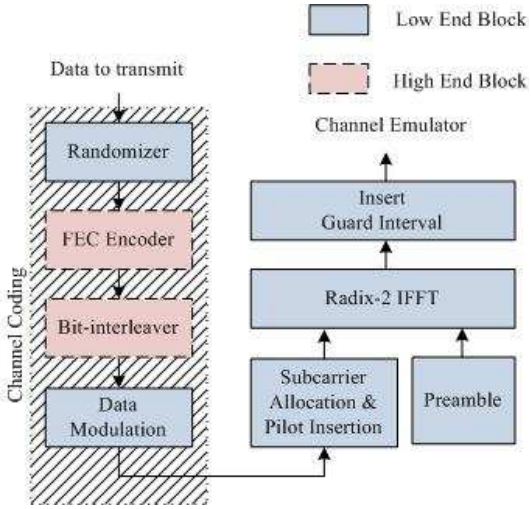

Fig. 3 OFDMA transmitter

Randomization:

The stage of randomization is to “whiten” the statistics of the data. It is performed by exclusive or operation on input binary data and the output of pseudorandom binary sequence with polynomial $1+x^{14}+x^{15}$.

Forward Error Correction:

To break up the burst bit error, the technique of interleaving should be added in with the convolutional code. It makes coding across the sub-carriers.

Interleaving:

Interleaver maps the adjacent coded bits to nonadjacent sub-carriers. Moreover, it maps the adjacent coded bits alternatively to less or more significant bits of constellation.

Data Modulation:

Quadrature phase shift keying (QPSK) is used for low-end implementation, and 16-quadrature amplitude modulation (16-QAM) for high-end implementation. The constellations are Gray-mapped.

OFDMA sub-carrier allocation and pilot insertion:

The OFDMA sub-carrier allocation strategy is: A fixed set of adjacent sub-carriers is used by user. Pilot sub-carrier are inserted in an OFDMA symbol with equal spacing and fixed position.

II. Receiver

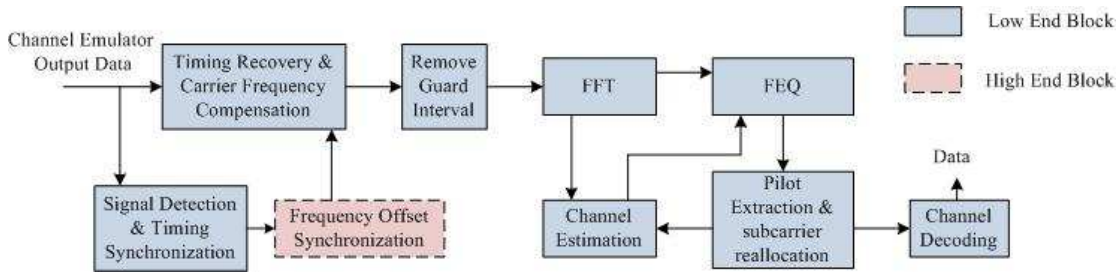

Signal Detection and Timing Synchronization

The first step of synchronization is to do timing estimation. The requirement here for estimate scheme is robust to frequency offset. The Schmidl and Cox algorithm provides such a robust estimation against to frequency offset.

Frequency Offset Synchronization

We use the method of M&M with appropriate modifications. The modification is to multiply the training symbol defined by timing estimator by its sign pattern. Then, the symbol is restored to possess the same structure which is proposed in M&M.

Channel Estimation

The knowledge of the channel characteristics is required. The ML channel response estimate can be realized by $\hat{\mathbf{h}} = \left[\mathbf{S}^H \cdot \mathbf{S}\right]^{-1} \mathbf{S}^H \cdot \mathbf{W}^H(\hat{v}) \cdot \mathbf{r}(0)$ We Assume that the channel response remains constant over at least one OFDM symbol interval.

C. Channel Emulation

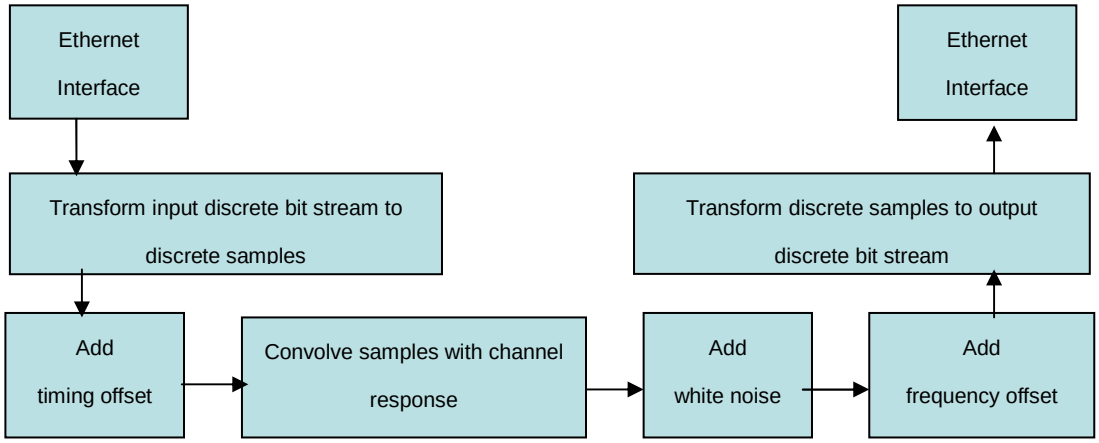

Generate NLOS/LOS block-variant fading channel to model outdoor wireless fixed wireless channel. Steps of low end channel simulator:

1. Received a block of discrete bit stream from the interface of transmitter, store the block.(a block is an/many OFDM symbol or 16e defined frame)
2. Convert the discrete input bit stream to discrete multilevel stream.
3. Generate a random time delay of the discrete multilevel stream.
4. Generate a random discrete type multi-path channel
5. Convolve the multilevel stream with generated multi-path channel.
6. Add noise to the processed multilevel stream.
7. Quantize and convert the quantized stream to discrete bit stream.
8. Send the discrete bit stream to the interface of receiver.

D. Audio/Video input/output (high-end)

1. Function in C: ***Input_video_process()***

   Description: Once the VDB driver decoder is opened *vDecOpen()* and configured *vDecConfig(arg1, arg2, arg3)*, the application only has to call *vDecGetFrame()* to obtain the most recently captured frame irrespective of whether a new frame has arrived since the last call of the API. Sub-functions

   vDecOpen()：Open the vDB Capture

   vDecConfig()：Configure the vDB Capture device

   vDecGetFrame()：get one captured frame from the vDB driver

2. Function in C: ***Output_video_process()***

   Description: Once the VDB encoder is opened *vEncOpen()* and configured *vEncConfig(arg1)*, the application only has to call *vEncSendFrame(arg1)* to pass the new frame to the VDB encoder to encode and display it, and obtain a free frame buffer where the application can write the next frame.

   vEncOpen()：Open the vDB display device

   vEncConfig()：Configure the vDB display device